99-227

Louisiana Transportation Research

Load Capacity of Hollowed Timber Piles

by

R. Richard Avent
Vijaya K. A. Gopu

LOUISIANA STATE UNIVERSITY

LTRC

Louisiana Transportation Research Center

Sponsored Jointly by Louisiana State University and the Louisiana Department of Transportation and Development

325

TECHNICAL REPORT STANDARD PAGE

1. Report No. **State Project Number: 736-99-0227**	2. Government Accession No.	3. Recipient's Catalog No.
4. Title and Subtitle **Load Capacity of Hollowed Timber Piles**	5. Report Date **December 1998** 6. Performing Organization Code	
7. Author(s) **R. Richard Avent, Ph.D., P.E.** **David J. Mukai, Ph.D.**	8. Performing Organization Report No. **325**	
9. Performing Organization Name and Address **Louisiana State University** **Department of Civil & Environmental Engineering** **Baton Rouge, LA 70803**	10. Work Unit No. 11. Contract or Grant No. **State Project Number: 736-99-0227** **LTRC Project Number: 95 – 4SS**	
12. Sponsoring Agency Name and Address **Louisiana Transportation Research Center** **4101 Gourrier Avenue** **Baton Rouge, LA 70809**	13. Type of Report and Period Covered **Final Report** **Period Covered: May 1995 – December 1998** 14. Sponsoring Agency Code	
15. Supplementary Notes		

16. Abstract

The goal of this study was to develop a reliable load-rating methodology for timber piles based on the level of documented damage. Louisiana currently has over 4,000 timber bridges in its inventory of over 13,800 bridges. A quarter of these 4,000 timber bridges are structurally deficient since they cannot support their design loads. One of the most common forms of deterioration is core decay resulting in a hollow pile with an undecayed outer shell. This outer shell may be solid or broken-up by vertical splits along the longitudinal axis of the pile. Pile deterioration may extend from a few feet up to the entire length of the pile.

Bridge maintenance personnel must make judgments on a regular basis as to the remaining capacity for these hollowed/decayed piles. Biennial inspections are routinely conducted for bridge substructures (every five years for underwater inspections). District bridge inspectors report visible defects and measure the thickness of the sound outer shell when decay is suspected. This data is then used to model the pile and perform a load rating analysis.

The Bridge Maintenance Section of DOTD supplied approximately 30 deteriorated timber piles up to ten feet (3 m) in length with a representative range of hollowness and splitting (checking). Small coupons were taken from most of the piles to determine the basic material properties. The degree of damage was quantified and each pile tested in axial compression. Mathematical models were developed to predict the axial load capacity and included all significant variables as typically reported by bridge inspectors. The theoretical and experimental results were compared to verify the model. Finally, recommended procedures were developed for load rating decayed timber piles.

The investigation has led to the following conclusions: (1) The strength of the sound wood portion of decayed piles is significantly lower than that of the new piles; (2) Piles having void areas less than 20 percent of the gross area tend to fail primarily by crushing; (3) Piles with void areas greater than 20 percent tend to fail primarily by buckling of the outer shell; (4) A good predictor of pile capacity is the energy required for a specific depth of radial penetration by a nail/probe into the pile; and (5) Based on this concept and a safety factor of three, equations were developed for predicting the pile allowable load for decayed timber piles.

17. Key Words timber, piles, decay, stiffness, compressive strength, pile capacity		18. Distribution Statement **Unrestricted. This document is available through the National Technical Information Service, Springfield, VA 21161.**	
19. Security Classif. (of this report) **Unclassified**	20. Security Classif. (of this page) **Classified**	21. No. of Pages	22. Price

Load Capacity of Hollowed Timber Piles

by
R. Richard Avent
Vijaya K. A. Gopu

Department of Civil & Environmental Engineering
Louisiana State University
Baton Rouge, Louisiana 70803

LTRC Project No. 95-4SS
State Project No. 736-99-0227

conducted for

LOUISIANA DEPARTMENT OF TRANSPORTATION AND DEVELOPMENT
LOUISIANA TRANSPORTATION RESEARCH CENTER

December 1998

ABSTRACT

The goal of this study was to develop a reliable load-rating methodology for timber piles based on the level of documented damage. Louisiana currently has over 4,000 timber bridges in its inventory of over 13,800 bridges. A quarter of these 4,000 timber bridges are structurally deficient since they cannot support their design loads. One of the most common forms of deterioration is core decay resulting in a hollow pile with an undecayed outer shell. This outer shell may be solid or broken-up by vertical splits along the longitudinal axis of the pile. Pile deterioration may extend from a few feet up to the entire length of the pile.

Bridge maintenance personnel must make judgments on a regular basis as to the remaining capacity for these hollowed/decayed piles. Biennial inspections are routinely conducted for bridge substructures (every five years for underwater inspections). District bridge inspectors report visible defects and measure the thickness of the sound outer shell when decay is suspected. This data is then used to model the pile and perform a load rating analysis.

The Bridge Maintenance Section of DOTD supplied approximately 30 deteriorated timber piles up to ten feet (3 m) in length with a representative range of hollowness and splitting (checking). Small coupons were taken from most of the piles to determine the basic material properties. The degree of damage was quantified and each pile tested in axial compression. Mathematical models were developed to predict the axial load capacity and included all significant variables as typically reported by bridge inspectors. The theoretical and experimental results were compared to verify the model. Finally, recommended procedures were developed for load rating decayed timber piles.

The investigation has led to the following conclusions: (1) The strength of the sound wood portion of decayed piles is significantly lower than that of the new piles; (2) Piles having void areas less than 20 percent of the gross area tend to fail primarily by crushing; (3) Piles with void areas greater than 20 percent tend to fail primarily by buckling of the outer shell; (4) A good predictor of pile capacity is the energy required for a specific depth of radial penetration by a nail/probe into the pile; and (5) Based on this concept and a safety factor of three, equations were developed for predicting the pile allowable load for decayed timber piles.

ACKNOWLEDGMENTS

The writers would like to acknowledge the contributions of the Bridge Maintenance Division of DOTD in supplying the test piles and providing assistance in the testing process. A special thanks goes to Joe Smith, Gil Gautreau, and Frank Castjohn.

Appreciation is also extended to Dr. Burl Deshongh formerly of LTRC, Walid Alaywan, and Art Rogers of LTRC for advice and coordination of the project.

IMPLEMENTATION STATEMENT

The product of this investigation is a methodology for determining the allowable stresses for damaged timber piles. Several alternatives are presented using various levels of approximation. Given that the degree of hollowness is known, the load capacity of the piles can be computed by the procedures described in this report. Consequently, the bent capacity can be computed from the aggregate pile summation.

The formulas provided using nail/probe approach should be considered preliminary due to the relatively small number of tests conducted with the probe. Before general adoption, the influence of the probe size should be evaluated so that this factor can be taken into account when determining the allowable stresses. The process also requires knowledge of the degree of hollowness of the pile. Available means for determining the minimum net area are limited. Additional research is needed to develop methods that can quickly determine net area.

TABLE OF CONTENTS

LIST OF TABLES

LIST OF FIGURES

INTRODUCTION

The goal of this study is to develop a reliable load rating methodology for timber piles based on the level of documented damage. Louisiana currently has over 4,000 timber bridges in its inventory of over 13,800 bridges. A quarter of these 4,000 timber bridges are structurally deficient since they cannot support their design loads, and over fifteen percent are functionally deficient since the traffic has outgrown the bridge's carrying capacity. Taking a conservative estimate of an average of four bents per bridge and four piles per bent means that there are over 64,000 timber piles supporting Louisiana bridges. Many of these bridges are over 40 years old, and bridge inspections routinely reveal pile deterioration. Of course, this problem is not unique to Louisiana only. Many states throughout the country have a large inventory of deteriorating timber pile bridges.

One of the most common forms of deterioration is core decay resulting in a hollow pile with an undecayed outer shell. This outer shell may be solid or broken-up by vertical splits along the longitudinal axis of the pile. Pile deterioration may extend from a few feet up to the entire length of the pile. The nature of this deterioration relates to the typical pressure treatment process, which strongly impregnates the outer shell, but provides little protection to the core. As long as the outer shell remains unbreached, decay is unlikely. Decay often results, however, from the growth of checks and splits in the outer shell, the holes made for connecting bracing and installing drift pins, and impact damage. The outer shell may be resistant to decay and remain solid for many years after the core is lost.

Bridge maintenance personnel must make judgments on a regular basis as to the remaining capacity for these hollowed/decayed piles. Biennial inspections are routinely conducted for bridge substructures (every five years for underwater inspections). District bridge inspectors report visible defects and measure the thickness of the sound outer shell when decay is suspected. This data is then used to model the pile and perform a load rating analysis.

A search of the literature revealed little information on the strength of hollowed timber piles. The literature primarily consisted of: (1) Growth of decay *[1]*; (2) Repair and rehabilitation *[2], [3], [4], [5], [6], [7], [8], [9], [10]*; and (3) Assessment of damages and deficiencies *[11], [12], [13], [14], [15], [16]*. No information was found on tests for remaining strength of old timber piles.

OBJECTIVES OF RESEARCH

Five categories determine the research objectives: quantification of damage, analytical procedures for predicting remaining strength, testing program, comparison of experimental and theoretical results, and development of a guide of recommended procedures:

Quantification of Damage

1. Evaluate typical field inspection data generated by DOTD during timber pile inspections.
2. Develop methodologies and procedures for quantifying damage in pile test specimens.
3. Develop procedures for quantifying basic material properties of test pile material.

Analytical Procedures for Predicting Remaining Strength

4. Formulate expected pile failure patterns and modes.
5. Develop mathematical models and evaluate key parameters and properties.

Testing Program

6. Develop a test protocol for measuring basic material properties of pile material.
7. Conduct a series of full-size tests.

Comparison of Experimental and Theoretical Results

8. Conduct comparison studies for each pile tested.
9. Modify analytical procedure for predicting remaining strength to obtain reliable strength values.

Recommended Guidelines

10. Develop a recommended DOTD guide describing the application of the load prediction procedure to determine the load rating (remaining capacity) of decayed piles.

SCOPE

The Bridge Maintenance Section of DOTD supplied approximately 30 deteriorated timber piles up to ten feet (3m) in length with a representative range of hollowness and splitting (checking). Small coupons were taken from each of the piles to determine the basic material properties. The degree of damage was quantified and each pile tested in axial compression. Mathematical models were developed to predict the axial load capacity and included all significant variables as typically reported by bridge inspectors. The theoretical and experimental results were compared to verify the model. Finally, a recommended procedure was developed for load rating decayed timber piles.

METHODOLOGY

Current procedures for DOTD pile inspection

Two types of inspections are conducted on timber piles in Louisiana. District inspectors inspect dry piles biannually. Dive teams under contract inspect piles in four feet or more of water underwater. Typical inspection procedures include: visual inspection, probing with ice pick or knife, and hammer soundings to detect hollow sections. When a hollow area is suspected, the typical procedure is to drive a series of spikes into the pile. The change in resistance is used to identify the degree of hollowness. An estimate of the size of the sound outer shell is thus obtained for the purpose of computing remaining capacity. Suspect areas may also be drilled or cored with an incremental borer. The degree of hollowness is measured by examining the core or by using a "feeler" gauge in the hole of the pile. Any exterior deterioration is measured and recorded. Based on an estimate of the reduced cross section, an allowable load is computed by multiplying the reduced cross sectional area times the allowable compressive stress.

Procedures for Quantifying Basic Material Properties of Test Pile Material

It is important to accurately evaluate the basic physical and mechanical properties of each test pile. The development of analytical procedures for predicting remaining strength of decayed piles will be partially based on data obtained in this phase of the project. The key physical properties are moisture content and density; and the key mechanical properties are compressive strength (parallel to the axis of the pile) and the corresponding modulus of elasticity.

The density of wood has a significant influence on its mechanical properties. This property can be determined from 2x2x8 inch (25 x 25 x 200 mm) specimens cut from the test piles and calculated as follows:

$$\text{Density} = \frac{\text{Weight of oven dry specimen}}{\text{Volume at original condition}} \qquad (1)$$

The density provides a measure of the amount of solid wood material in the outer shell of the test piles and may explain any variation in the mechanical properties of the solid outer shell.

The moisture content of wood also influences its mechanical properties, primarily due to its effect on volume.

The moisture content of the test piles can be determined simultaneously with the density if 2x2x8 inch 25 x 25 x 200 mm) specimens are used in lieu of the ASTM D143 specimen, which are 2x2x1 inches (25 x 25 x 100 mm). The moisture content is computed as:

$$\text{Moisture Content (percent)} = \frac{\text{Original Weight - Weight Oven Dry}}{\text{Weight Oven Dry}} \times 100\% \qquad (2)$$

The compressive strength (parallel to grain) and modulus of elasticity of the undecayed outer shell material of the pile was determined using small blocks, 2x2x8 inches (25 x 25 x 200 mm), oriented in the pile axis direction, and loaded to failure in compression. This test is the standard ASTM D-143. A minimum of two samples was taken from each pile, but more were taken if enough solid material was available. The test coupons were loaded with a head movement rate of 0.05 inch/minute (1.27 mm/mm) until the peak load had been reached. After the peak load had been reached, the machine head movement was stopped for a minute or so to view the relaxation. The testing was resumed with a head movement rate of 0.2 inch /minute (5 mm/min.) until the coupons failed. The modulus of elasticity parallel to grain was obtained from the experimental load versus deformation data.

Pile Selection and Damage Evaluation

Approximately 30 piles were provided by DOTD, which were suitable for testing. A few additional piles had deteriorated to an extent that testing could not be conducted. All but one of the piles was taken from old bridges and had significant deterioration. One undamaged new pile was also provided for comparison purposes. Two piles were long enough that both a hollow section and a relatively solid section could be cut from the same pile. Each piece was tested separately.

Because the slenderness ratio, l/r, was small (around 14 for the worst cases), Euler buckling was not a consideration in these pile tests. It was therefore necessary to have flat bearing surfaces perpendicular to the longitudinal axis of the pile. To prepare the end surfaces for testing, the piles were cut using a cross cut saw. A large miter box was constructed to cut up to a seven-foot (2.1 m) long test specimen. Each pile was leveled and secured in the miter box prior to cutting to length. Both ends were cut without moving the pile to insure that the ends were even and parallel. The process of cutting a pile in the miter box is shown in figure 1.

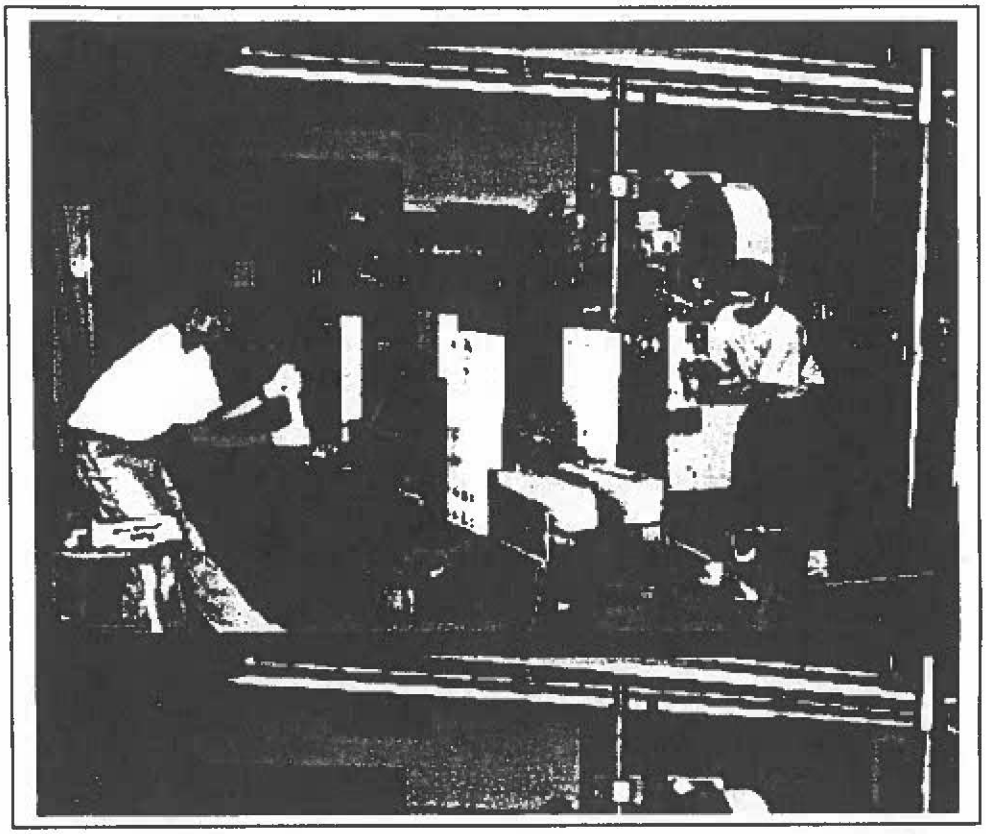

Figure 1
Cross cut sawing of pile in miter box to prepare end sections for loading

The pieces cut off at the end of each test pile were used to obtain solid clear wood coupons. These coupons were later tested to determine basic mechanical properties, specifically, compression strength parallel to grain and modulus of elasticity. The coupons were prepared and tested according to ASTM -D695. The coupons were approximately 2x2x8 inch (51x51x203mm) long. The number of coupons taken from each pile varied from two to twelve. Since all coupons were taken from the solid wood portion of the cut off sections, only a limited number of coupons could be obtained from the more heavily decayed piles.

Prior to testing each pile, a detailed inspection was made. Circumferences were measured at one-foot intervals and all surface damage was noted. In addition, the cross sections at each finished end were traced for later quantification of the amount of decay. A detailed evaluation of the exterior of each pile is given in the appendix.

A summary of the more significant characteristics is given in table 1. The amount of checking is classified as: (1) light - few; small, shallow checks; (2) moderate - small, shallow checks; (3) heavy - many checks spaced at less than one inch (25 mm) with numerous deep checks. Deep checks are those greater than ½ inch (12 mm) deep. The pile test specimens varied in length from two to seven feet (0.6 - 2.1 m) with most being hollow to varying degrees.

After the testing was completed, the piles were cut, (generally in one foot [0.3m], increments) to measure the variation in cross section over the length of the piles. The variation in cross sectional area is graphically shown for four representative piles in figures 2-5. The hollow areas of the test piles ranged from approximately 40 percent to 0 percent of the gross area. The length of the voids varied from pile to pile. While some cross sections exhibited an outer shell of relatively uniform thickness, the more typical case was that of a highly irregular shell thickness. The exterior of the test piles generally had a few knots, small holes, and small scarfs. The degree of splitting and checking varied from light to heavy. A few piles had large splits, which penetrated the full thickness of the outer shell and produced an open section. The significance of these conditions is discussed in a later chapter that analyzes the results.

Nail Penetration Energy for Deteriorated Piles

Prior to testing the piles to failure, a select group of piles was evaluated for nail penetration energy characteristics. This was accomplished by driving a large diameter nail radially into the pile using an universal testing machine and determining the energy required to drive the nail for a depth of one and two inches into the pile. This penetration energy provides a measure of the compressive strength of the woodpile in service. The greater the pile deterioration, the lower the penetration energy for a given penetration depth. A typical nail force versus penetration curve obtained for a pile is shown in figure 6.

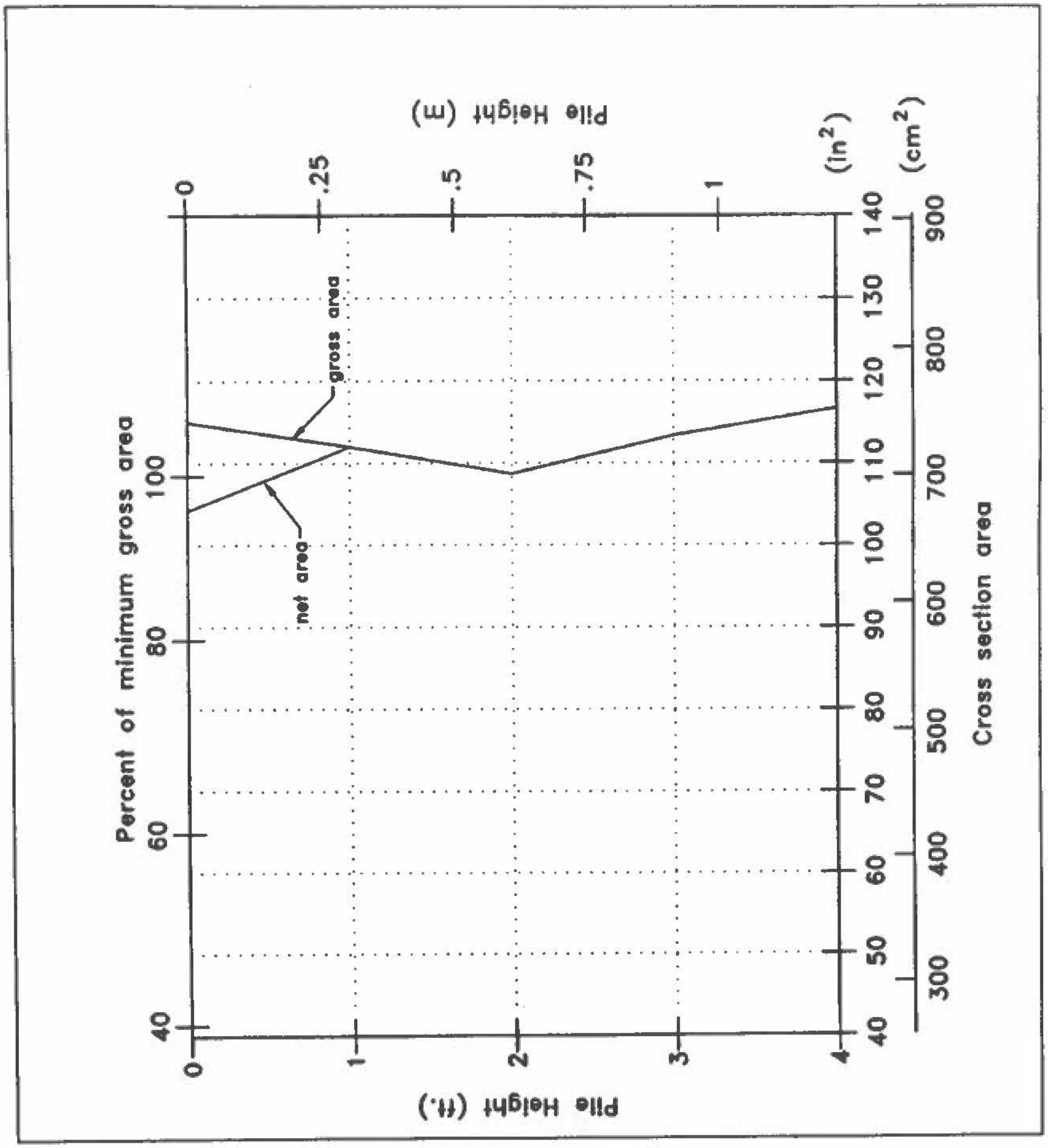

Figure 2
Variation in cross section area for pile 3A

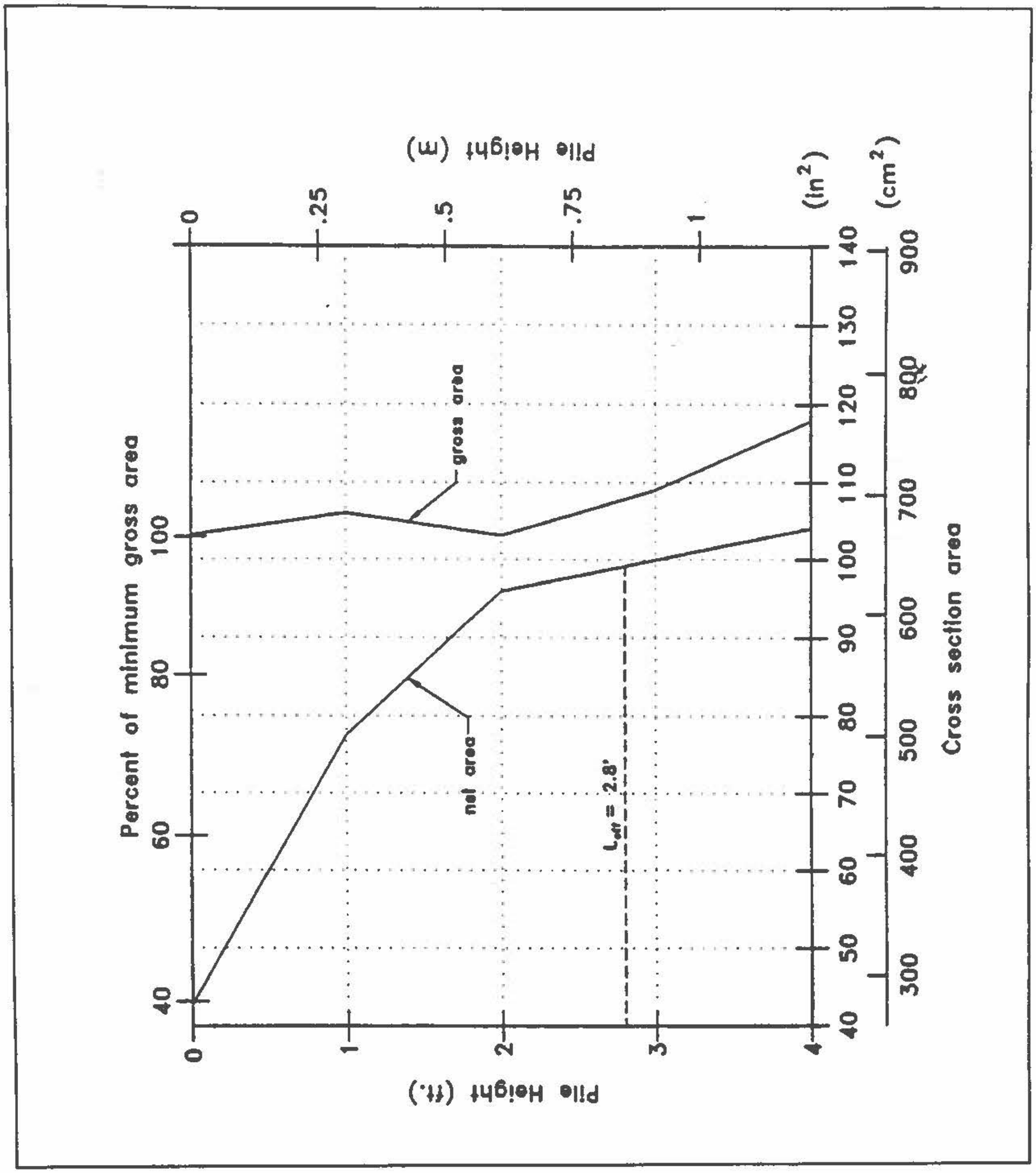

Figure 3
Variation in cross section area for pile 3B

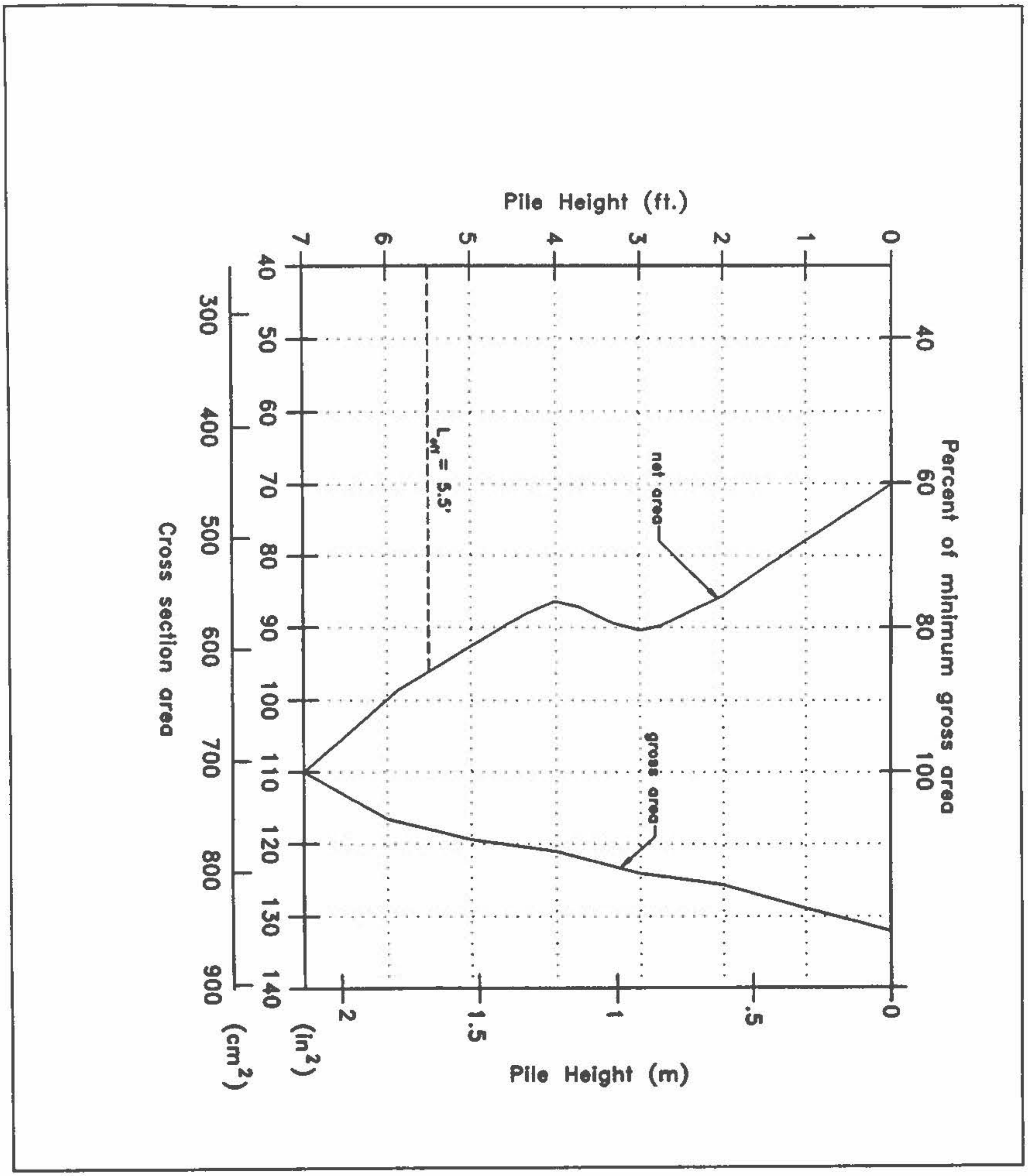

Figure 4
Variation in cross section area for pile 4

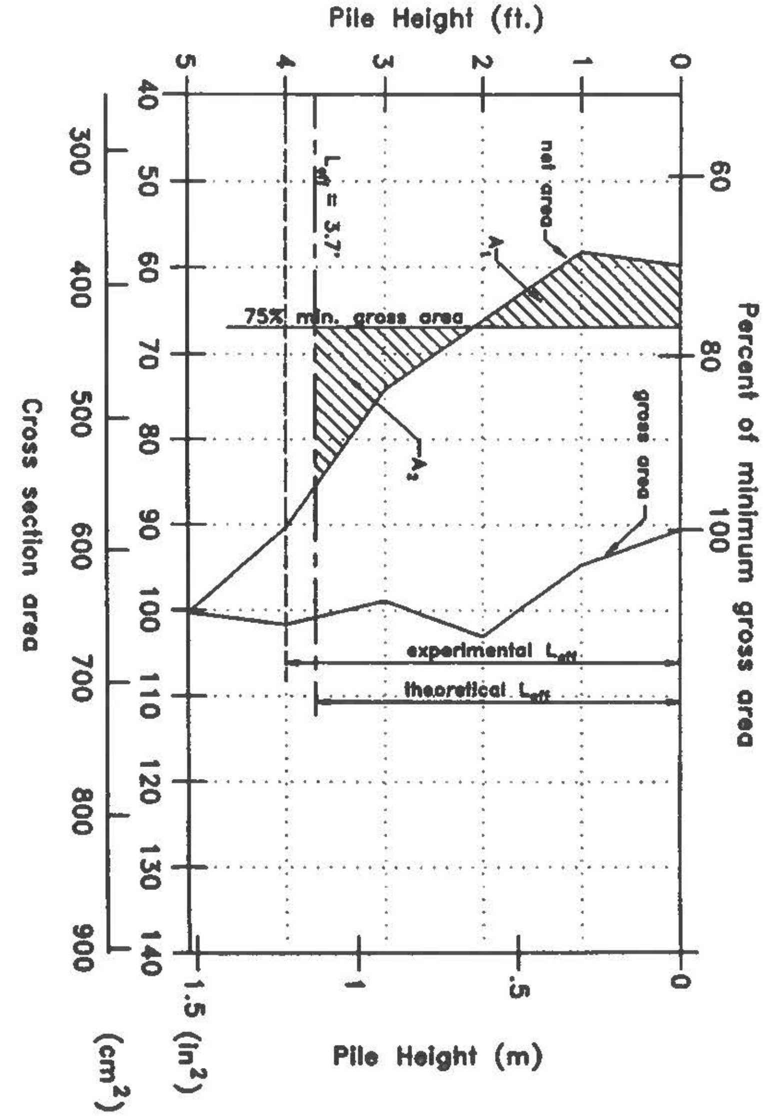

Figure 5
Variation in cross section area for pile 5

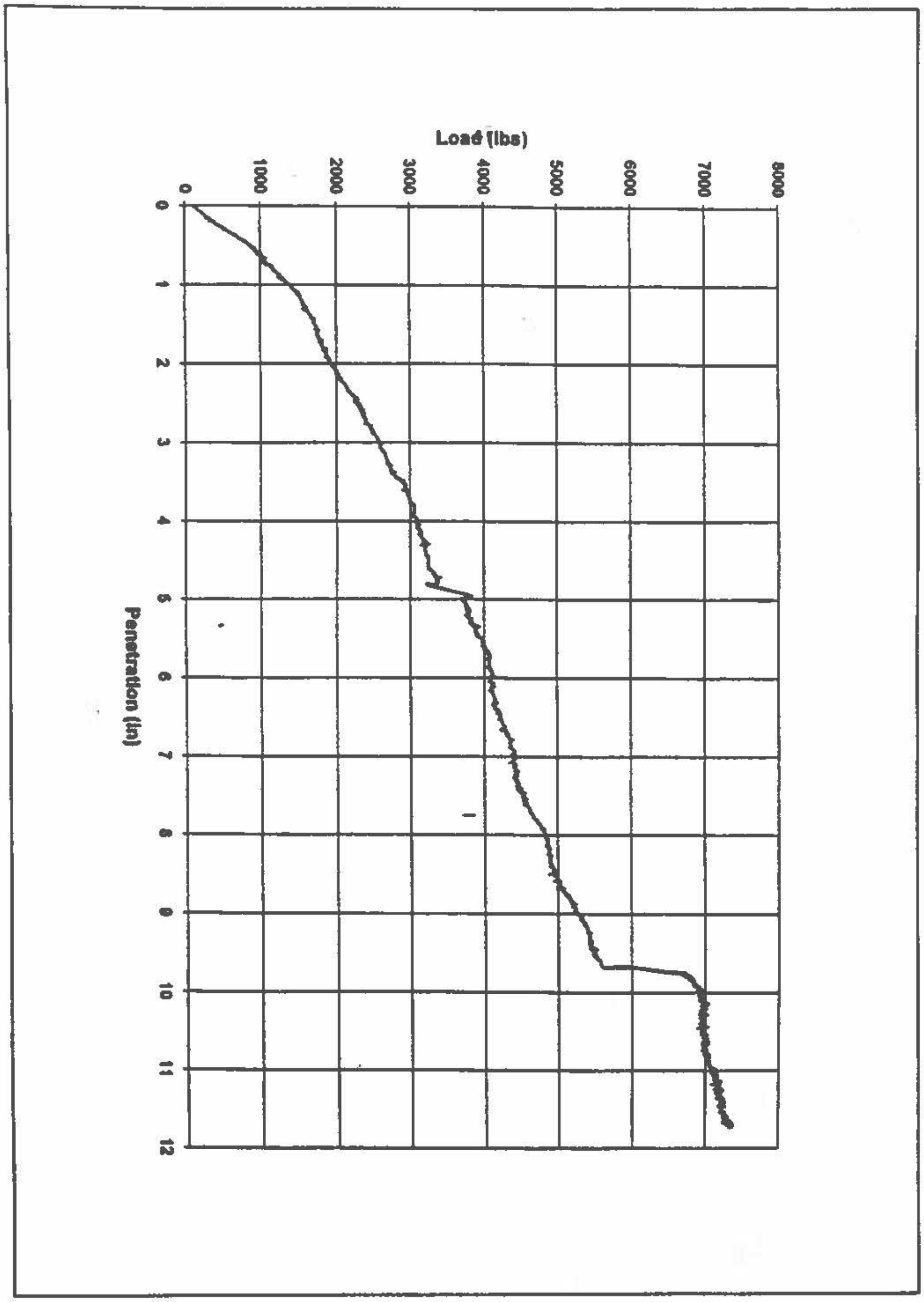

Figure 6
Load vs. penetration of nail in pile No. 29

Table 1
Visual evaluation of each test pile tested

Pile No.	Pile Length (in.)	Cross Section Area (in^2)				Degree of Checking	Other Characteristics
		Gross Area		Net Area			
		Top	Bottom	Top	Bottom		
3A	48	115.0	116.5	103.7	116.5	Heavy	Solid but 1" outer shell partially delaminated from core
3B	51	103.1	117.9	42.7	105.3	Moderate-Heavy	Hollow over full length
4	84	132.1	110.0	70.7	110.0	Heavy-light	Hollow in upper section and solid in lower section with large split from top to 49" long with maximum width of 3" and depth of 4"
5	60	90.6	100.3	59.9	100.3	Heavy	Top section hollow and bottom section solid with large split in top third of shell
6	59.5	155.9	138.7	99.5	47.5	Heavy	Hollow from top to bottom with outer shell decay on top 12"
7	72	110.5	121.0	110.5	121.0	Heavy	Solid throughout but outer 2" shell delaminated from core
8A	79.5	116.5	142.1	92.0	92.0	Moderate	Hollow over full length with portion of shell decayed at top with two 5' long splits having maximum width of 1/2"
8B	26.75	113.5	116.5	89.2	116.5	Moderate	Hollow top and solid bottom with outer shell decay on top 12"
9	55	121.0	136.8	121.0	136.0	Light	Solid undamaged pile
10	48	112.5	129.7	55.6	99.3	Light	Hollow over full length with 2" wide by 12" long opening in the shell at the top
11	60	113.3	122.7	75.6	122.7	Light	Hollow at the top and solid at bottom with 25" long, 1/2" wide crack in shell at the top
12	84	123.3	132.9	72.6	132.9	Heavy	Hollow at the top and solid at bottom with crack 1/2" wide and 25" long at top
13	83.75	128.9	115.6	106.6	108.6	Moderate	Hollow over full length with small reduction in section at the bottom
14	60	109.1	99.8	74.4	99.8	Moderate-Heavy	Hollow in Center
15	60	102.6	113.7	102.6	94.6	Moderate-Heavy	Fairly solid

Table 1
Visual evaluation of each test pile tested (cont'd)

Pile No.	Pile Length (in.)	Cross Section Area (in^2)				Degree of Checking	Other Characteristics
		Gross Area		Net Area			
		Top	Bottom	Top	Bottom		
16	60	115.3	108.7	103.1	108.7	Moderate-Heavy	Fairly solid
17	60	114.1	113.3	94.8	113.2	Moderate-Heavy	Cracked shell and hollow
18	60	102.8	101	93.9	101	Moderate-Heavy	Fairly solid
19	72	100.1	110.4	100.1	110.4	Moderate-Heavy	Outer hollowness
20	72	118.8	113.1	96.9	113.1	Moderate-Heavy	Hollow in center
21	48	103.9	108.2	90.8	105.9	Moderate-Heavy	Hollow in center
23	72	141.2	192	120.1	91.2	Moderate-Heavy	Cracked shell and hollow
24	72	100.3	123.4	81.7	107.4	Moderate-Heavy	Hollow in center
25	48	116.2	105.2	54.3	105.2	Moderate-Heavy	Very hollow in center
26	72	120.1	86.4	120.1	86.4	Moderate-Heavy	Outer shell open and very hollow in center
27	72	91.1	77.2	91.1	76.8	Moderate-Heavy	Outer shell open and very hollow in center
28	72	83.9	148.6	83.9	83.7	Moderate-Heavy	Solid at top and hollow in center at bottom
29	72	111.7	148.1	111.7	148.1	Moderate-Heavy	Solid
30	72	96.1	145.1	96.1	144.9	Moderate-Heavy	Fairly solid
32	72	118.1	177.8	118.1	161.1	Moderate-Heavy	Fairly solid

Results of pile tests

Testing protocol. The evaluation and preparation of the test piles have already been described. Each pile was load tested in a 550 K (2,448KN) capacity MTS servo-hydraulic testing machine. The tests were conducted at a constant loading head travel rate of 0.015 inch/minute (0.38 mm/min). Both displacement and load values were automatically recorded at one-second intervals.

Pile test results. A summary of the test results is given in table 2. A more detailed description of each pile failure as well as all test results are given in appendix III. The failure patterns fell into four categories: (1) crushing; (2) shell buckling; (3) combined shell buckling and twisting; and (4) shell buckling with solid core crushing.

Crushing. For relatively short piles in which Euler buckling does not occur, the most typical failure pattern is crushing. Pile 8B exhibited this failure pattern and is shown in figure 7 after failure had occurred. This pile was short (approximately 27 inches [686 mm]) and relatively solid except for some decay near the top. There was slight flaring near the top (see top right side of the pile in fig. 7). However, the failure was primarily one of crushing.

Shell buckling. Most of the piles had a significant length of hollow cross section. The outer shell typically ranged from one to four inches (25-100mm) in thickness. In addition, checking had occurred on all piles with many having a heavy check pattern. As these piles were loaded, hoop stresses were generated and the outer shell bulged radially outward. The outer shell of these piles split longitudinally at these checks as loading progressed. With the degree of checking present in these piles, the perpendicular-to-grain tension resistance is minimal. As a result, a pile becomes subdivided into a series of parallel slender columns having cross section dimensions equal to the shell thickness and the spacing between the checks penetrating the shell (typically 1-3 inches [25-76 mm]). These slender column segments cannot buckle inward because of the adjoining shell segments. Therefore, when the loads produce an unstable equilibrium condition, the segments buckle outward. Pile 6 displays a typical example of this behavior (fig. 8). The bulging and separation of the segments at the checks can be clearly seen. Most of the piles failed in this manner (table 2).

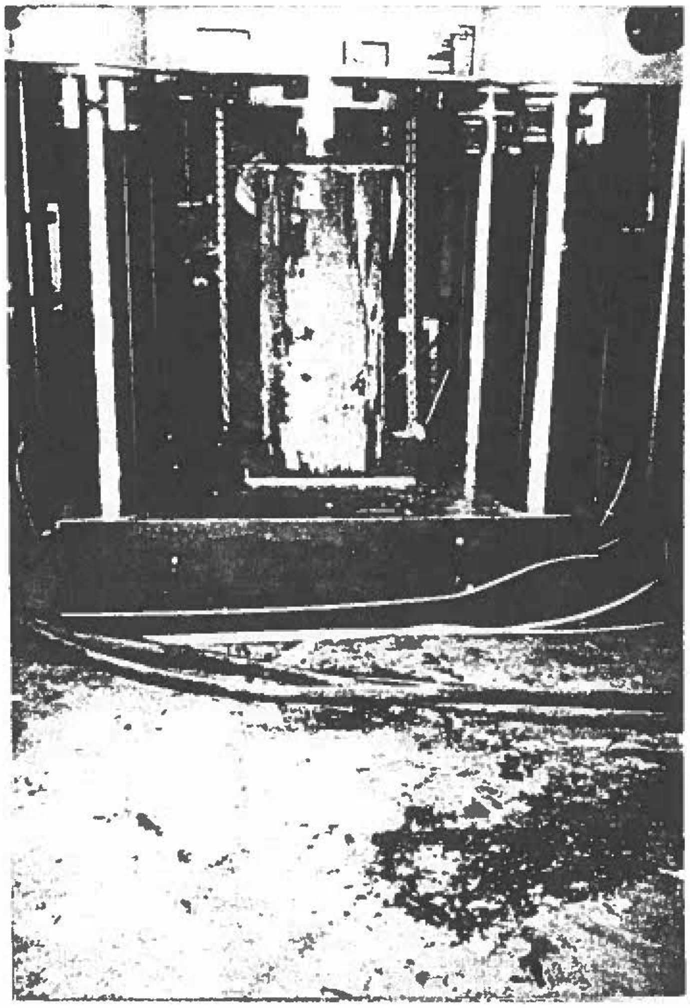

Figure 7
Example of crushing failure in Pile 8B

Table 2
Summary of pile test results

Pile No.	Pile Length (in.)	Outer Shell Buckling Length (in.)	Minimum Cross Section Area (in^2)[1]		Ultimate Load (lbs)	Ultimate Compressive Stress (psi)		Failure Pattern
			Gross Area	Net Area		Based on Gross Area (F_{cn})	Based on Net Area (F_{cn})	
3A	48.0	0.0	104.2	108.7	183,600	1,689	1,762	Outer 1" shell buckled and solid core crushed
3B	51.0	24.0	42.7	103.1	84,100	816	1,970	Outer 1" shell buckled over bottom 24" length and core crushed
4	84.0	24.0	70.7	110.0	191,300	1,739	2,706	Upper 24" of hollow shell buckled
5	60.0	48.0	59.9	90.6	55,200	609	921	Shell buckled and twisted over most of length
6	59.5	48.0	48.3	138.7	126,000	908	2,608	Shell buckled Shell buckled over all but top 1 foot
7	72.0	0.0	110.5	110.5	131,200	1,188	1,188	Primarily crushed with lower shell buckling
8A	79.5	79.5	92.0	116.5	98,800	848	1,074	Shell buckled over most of length
8B	26.75	0.0	89.2	113.5	210,400	1,854	2,359	Primarily crushed
9	55.0	0.0	121.0	121.0	470,800	3,891[3]	3,891[3]	Did not fail-exceeded machine capacity
10	48.0	24.0	55.6	112.5	150,900	1,342	2,715	Shell buckled in upper section
11	60.0	24.0	73.1	113.3	265,000	2,339	3,625	Shell buckled and twisted over top 2 feet
12	84.0	56.0	72.6	121.7	94,300	775	1,299	Shell buckled over middle 2/3 of length
13	83.75	63.0	106.6	115.6	67,000	579	628	Shell buckled over upper 3/4 of length

Table 2
Summary of pile test results (cont'd)

Pile No.	Pile Length (in.)	Outer Shell Buckling Length (in.)	Minimum Cross Section Area (in^2)[1]		Ultimate Load (lbs)	Ultimate Compressive Stress (psi)		Failure Pattern
			Gross Area	Net Area		Based on Gross Area (F_{cn})	Based on Net Area (F_{co})	
14	60	48	112.01	74.353	231,981	2,071	3,120	Shell buckled and core crushed
15	60	60	109.66	93.673	271,839	2,479	2,902	Crushed with partial shell buckling
16	60	36	118.72	103.15	390,956	3,293	3,790	Crushed with lower shell buckling
17	60	60	121.04	78.531	164,130	1,356	2,090	Outer shell buckled over most of length
18	60	60	108.19	94.003	269,507	2,491	2,867	Crushed with upper shell buckling
19	48	48	108.21	99.111	304,171	2,811	3,069	Crushed with partial shell buckling
20	72	72	122.58	92.768	215,871	1,761	2,327	Shell buckled in mid-section
21	48	48	110.40	90.917	250,839	2,272	2,759	Shell buckled and twisted at top
23	72	72	164.81	91.339	60,649	368	664	Outer shell buckled
24	72	72	109.63	70.252	66,107	603	941	Shell buckling over middle 2/3 length
25	48	36	112.76	54.332	40,369	358	743	Shell buckling over full length
26	72	72	133.71	86.467	56,290	421	651	Outer shell buckled and core crushed
27	72	72	106.05	76.828	74,446	702	969	Shell buckling
28	72	48	94.726	83.793	95,105	1,004	1,135	Primarily crushed
29	72	24	124.14	111.73	450,259	3,627	4,030	Crushed and partial shell buckling

Table 2
Summary of Pile Test Results (cont'd)

Pile No.	Pile Length (in.)	Outer Shell Buckling Length (in.)	Minimum Cross Section Area (in^2)[1]		Ultimate Load (lbs)	Ultimate Compressive Stress (psi)		Failure Pattern
			Gross Area	Net Area		Based on Gross Area (F_{cu})	Based on Net Area (F_{cu})	
30	72	72	116.42	96.069	114,322	982	1,190	Primarily crushed with lower shell buckling
32	72	48	147.09	118.13	196,804	1,338	1,666	Shell buckled and twisting at top
					Average	1,223[3]	1,902[3]	

[1] May occur at locations other than the top and bottom of the pile.
[2] Pile did not fail and loading terminated at 470,800 lbs.
[3] Pile 9 results not included in determining average values.

Note: 1 in. = 25.4 mm
1 lb. = 4.45 N
1 psi = 6.89 kPa

Figure 8
Example of shell buckling failure in pile 6

Combined shell buckling and twisting. In two instances the shell buckling was accompanied by torsional rotation about the longitudinal axis of the pile (fig. 9). Such behavior results when piles have large splits with gaps creating an open section, which is weak in torsion. Piles 5 and 11 exhibited this pattern of failure.

Shell buckling with solid core crushing. Several piles were solid with no significant decay. However, the outer shell had begun to delaminate from the solid core. During loading of these piles, the outer shell buckled. The solid core continued to resist an increasing load until a crushing failure occurred. Pile 3A is a typical example of this behavior (fig. 10).

Coupon test results. A variable number of coupons were taken from the test piles to determine the clear wood ultimate compression stress. The results are shown in table 3. Excluding pile 9 coupons, the average ultimate stress is 2,816 psi (19,403 kPa). The coupons from pile 9 averaged values over 60 percent higher. It is apparent that even the "solid" wood in the piles has deteriorated with time. The average compressive strength of the coupons taken from the piles was reflective of the condition of the wood material in the pile. Figure 11 shows a plot of coupon stress at failure versus the pile stress at failure and clearly demonstrates the strong correlation between the two properties.

Modulus of elasticity. A value of the modulus elasticity can be estimated from the pile tests. Converting the load-deformation curves to stress-strain curves, the linear portion of these curves provides an estimate (or average) of the modulus of elasticity. The value is an estimate because: (1) the cross section area varies over the pile length due to pile taper and decay, thus an average area must be used when converting load to stress; (2) the P-< effect should be small in the linear portion of the curve; and (3) the strain is averaged over the entire length of the pile. The values of the modulus of elasticity are shown in table 4. The results illustrate another disadvantage of deteriorated piles--the stiffness has significantly reduced.

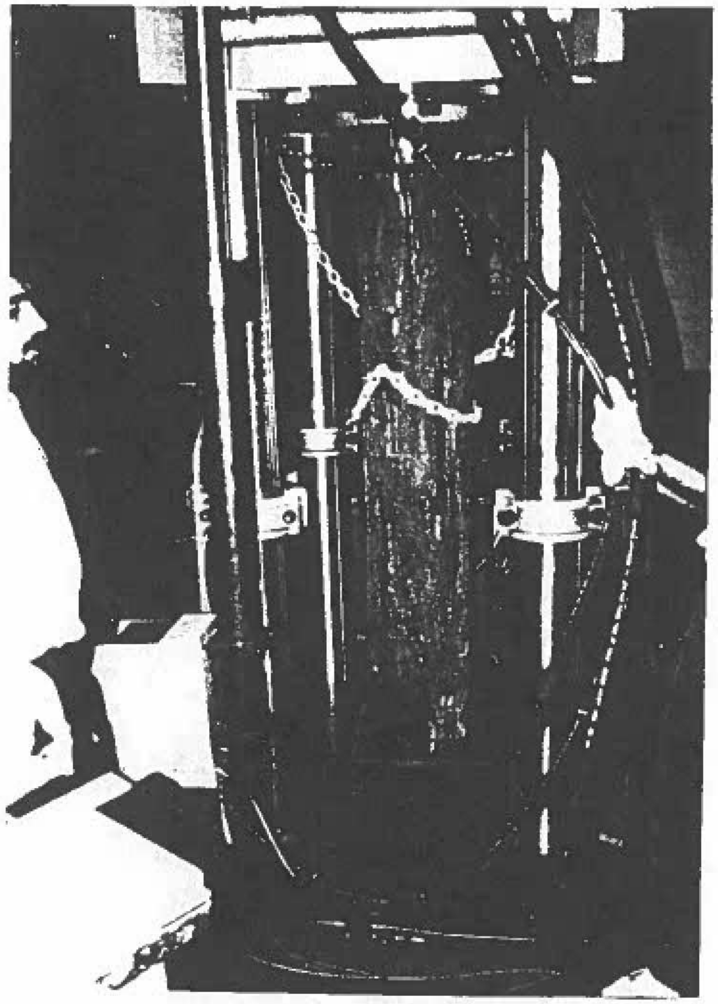

Figure 9
Example of combined buckling and twisting in pile 5

Figure 10
Example of combined buckling and crushing in pile 2

Table 3
Results of coupon Compression Tests

Pile Number	Number of Coupons	Avg. Ult. Comp. Stress (psi)
3	2	1769
4	4	3225
5	2	2728
6	3	3003
7	3	3097
8	6	2824
9	6	4679
10	3	4321
11	4	7547
12	5	4687
13	5	2201
14	11	4288
15	9	3222
16	15	4408
17	12	4699
18	9	4014
19	12	5094
20	11	4093
21	11	4136
23	13	2217
24	5	3150
25	11	2879
26	8	2568
27	11	2587
28	11	2226
29	11	5309
30	9	2169
32	9	2287

Note: 1 psi = 6.89 kPa

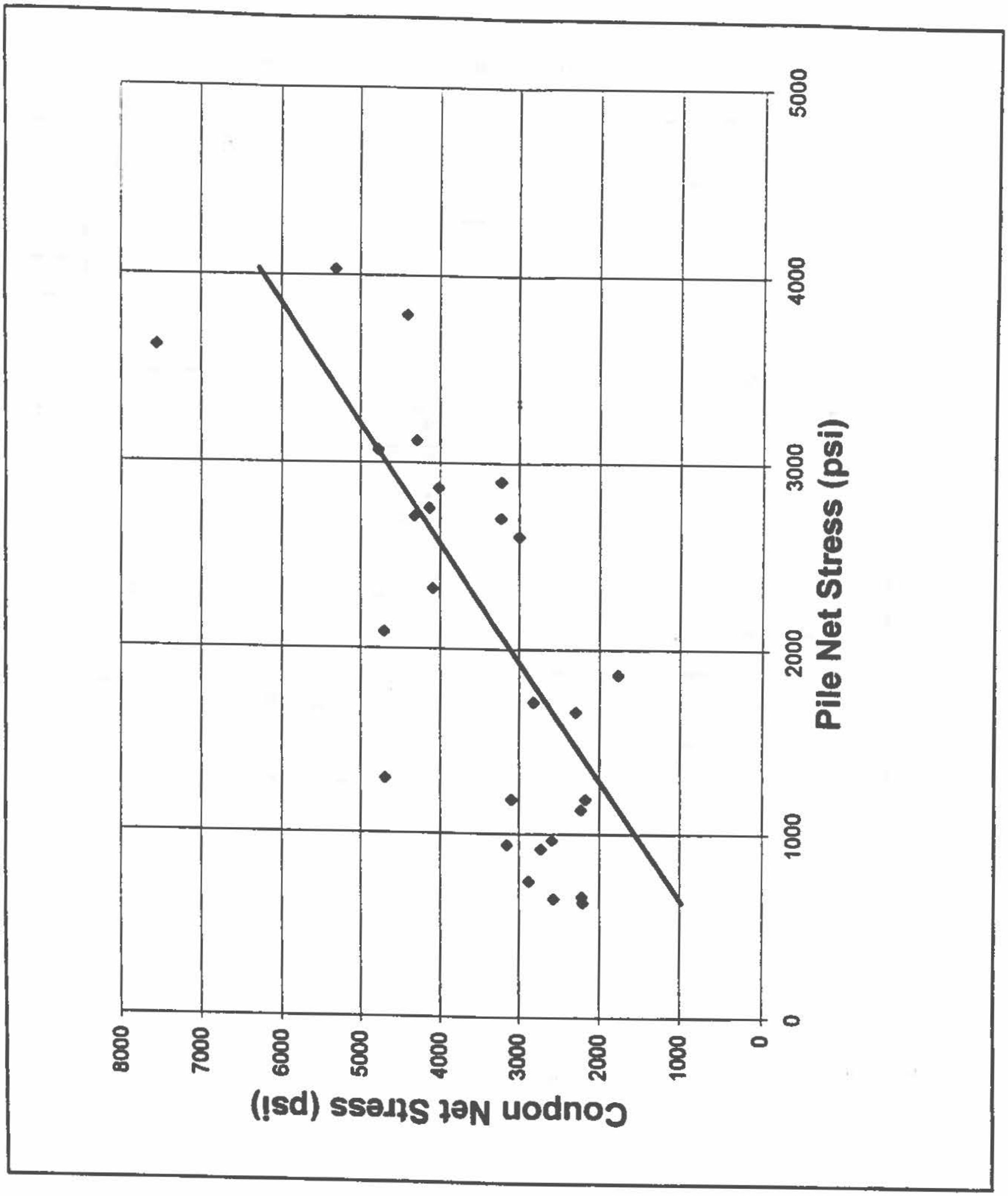

Figure 11
Average failure stress of coupons versus net failure of corresponding piles

Table 4
Approximate modulus of elasticity for test piles

Pile No.	Average Cross Section Area (in^2)	Pile Length (in)	Modulus of Elasticity (psi)
3A	81.25	48	548,000
3B	74.00	51	476,200
4	89.85	84	744,700
5	84.50	60	311,100
6	73.52	59.5	672,800
7	115.75	72	341,700
8A	104.23	79.5	280,000
8B	102.82	26.75	383,300
9	129.00	55	912,500
10	77.45	48	493,800
11	99.80	60	585,100
12	102.64	84	485,700
13	107.60	83.75	370,600
14	87.1	60	746,374
15	98.6	60	796,414
16	105.9	60	952,009
17	104	60	612,984
18	97.5	60	894,835
19	105.25	72	957,576
20	105	72	900,139
21	98.35	48	756,151
23	105.65	72	209,986
24	94.55	72	334,324

25	79.75	48	111,062
26	103.25	72	371,030
27	83.95	72	436,920
28	83.8	72	425,790
29	129.9	72	844,440
30	120.5	72	437,177
32	139.6	72	477,136
		Average	474,417

[1] Excluding pile No. 9; Note: 1 inch = 25.4 mm; 1 psi = 6.89 kPa

DISCUSSION OF RESULTS

Factors Influencing Pile Strength

The test results provide guidance as to the most significant factors affecting the strength of damaged piles. The importance of these factors is discussed in the following sections.

Strength of solid wood in decayed piles

The ultimate load capacity of the decayed piles was significantly reduced. The average ultimate compressive stress value, based on the gross area, approximately equals the allowable compression stress of 1,200 psi (8,628 kPa) as given in the National Design Specification (NDS) for Wood Construction [17]. However, one-half of the 30 piles had values significantly lower than 1,200 psi (8,268 kPa). If the net section is considered, the average stress is somewhat higher, 1,902 psi (13,105 kPa), but still quite low. For example, considering a safety factor of 2.25, the expected ultimate stress would be 2,700 psi (18,600 kPa). The ultimate stress in pile 9, the new undamaged pile, exceeded 3,950 psi (27,200kPa). Hence, by any measure these ultimate stresses are low. The key for deciding if, and/or when, to replace a damaged pile is to predict the remaining strength in an existing pile.

It has generally been assumed that the solid wood portion of a decayed pile retains its original design strength. Consequently, the normal procedure for evaluating the strength of damaged piles is to take the product of the allowable design stress, F_a, and the net area, A_n, that is,

$$P_{all} = F_a A_n \qquad (3)$$

where P_{all} is the allowable compressive load on the pile.

However, the results of this investigation indicate that the design allowable stress, F_{all}, for the solid portion of the pile does not remain constant. Rather, the strength decreases over time. Various factors that influence pile strength were considered in this study and are discussed in this section.

Degree of Checking

For piles with hollow sections, buckling of the outer shell is the typical failure mode. This behavior is a function of the degree of checking. In order to quantify the checking patterns, the end cross sections of piles 3-32 were examined and the number of checks greater than one half inch counted. The piles were than rated for checking using the following criteria:

Rating	Total Checks at Both Ends Greater Than ½in. (13 mm)
Light	10 or less
Moderate	11 - 19
Heavy	20 or more

The checking ratings for all hollow piles (solid piles were excluded) are shown in table 5. The piles are listed in ascending order of ultimate stress on the net section. The correlation between checking and pile capacity is weak. There is a trend of the most lightly checked piles being stronger. However, there is no distinction in the moderate to heavily checked beams. Based on these results, the degree of checking does not appear to be a good predictor of pile capacity.

Geometric Properties of Hollow Sections

The failure pattern of the hollow piles involved a buckling component. However, the irregularity of the hollow pile geometry makes it difficult to quantify this behavior. Several factors which may significantly influence the strength include: symmetry of the hollow section, whether the hollow section is open or closed; variation in outer shell thickness; and variation in size of the hollow core over length. As a result of these factors, a pile may exhibit one of three failure patterns:

1. Elastic buckling of the outer shell
2. Crushing of pile without buckling
3. A combination of crushing of the core and buckling of the outer shell

A summary of the geometric properties for the piles tested is given in table 6. Each pile is classified as to whether it is a solid section or hollow (open or closed) section. Note that most of the open sections are due to a deep check penetrating the shell. However, three of the piles had decay in the outer shell, which produced a gap rather than a check.

During testing, the approximate length of the buckled section was recorded. Most of the piles only buckled over a portion of their total length due to variations in cross section area. This length, l_{eff}, is referred to as the effective length and is a function of the variation of the hollow cross section over the pile length.

Table 5

Comparison of the failure stress based on average net cross section area to degree of checking for hollow piles

Pile Number	F_{net} (psi)	Checking
13	328	Moderate
24	399	Moderate-Heavy
25	506	Moderate-Heavy
26	545	Moderate-Heavy
23	571	Moderate-Heavy
27	887	Moderate-Heavy
5	921	Moderate
30	949	Moderate-Heavy
8A	1074	Light
28	1135	Moderate-Heavy
12	1299	Heavy
32	1410	Moderate-Heavy
17	1578	Moderate-Heavy
3B	1970	Heavy
20	2056	Moderate-Heavy
21	2550	Moderate-Heavy
6	2608	Heavy
14	2663	Moderate-Heavy
4	2706	Moderate
10	2715	Light
15	2757	Moderate-Heavy
18	2764	Moderate-Heavy
19	2890	Moderate-Heavy
29	3466	Moderate-Heavy
11	3625	Light
16	3692	Moderate-Heavy

Note: 1 psi - 6.89 kPa

Table 6
Geometric Properties of Pile Cross Sections

Pile Number	Section Type	Pile Length (in.)	Observed length of shell buckling (in.)	Theoretical length of shell buckling (in.)
3A	Solid	48	0	0
3B	Hollow/closed	51	24	18
4	Hollow/open	84	24	66
5	Hollow/open	60	48	42
6	Hollow/closed	59.5	48	59.5
7	Solid	72	0	0
8A	Hollow/open	79.5	79.5	79.5
8B	Hollow/open	26.75	0	0
9	Solid	55	0	0
10	Hollow/open	48	24	30
11	Hollow/open	60	24	40
12	Hollow/closed	84	56	40
13	Hollow/open	83.75	63	54
14	Hollow/closed	60	48	30
15	Hollow/closed	60	60	42
16	Hollow/closed	60	36	0
17	Hollow/open	60	60	48
18	Hollow/closed	60	60	0
19	Hollow/closed	72	48	0
20	Hollow/closed	72	72	36
21	Hollow/closed	48	48	21
23	Hollow/open	72	72	72
24	Hollow/open	72	72	54
25	Hollow/closed	48	36	24
26	Hollow/open	72	72	54
27	Hollow/closed	72	72	54
28	Hollow/open	72	48	18
29	Hollow/closed	72	24	0
30	Hollow/closed	72	36	12
32	Hollow/closed	72	48	12

Computation of pile capacity based on net area

The simplest approach to estimate pile capacity is to develop an allowable stress based on the net cross section (equation 1). The location of the net section is typically found using hammer soundings. The thickness of the solid shell is then measured by drilling holes then measuring with a "feeler" gauge or by driving nails until resistance is decreased and measuring the nail length.

The determination of the allowable stress can be based on the data from this study. The sample of 30 piles is too small for a meaningful statistical analysis. However, a value can be estimated that provides a margin of safety. The average failure stress on the net section of all damaged piles was 1,902 psi (13,100 kPa), and the lowest value was 628 psi (4,330 kPa). A conservative approach would be to use a safety factor of two (2) on the lowest test value, which that would give all allowable stress (rounded to the nearest 50 psi) of

$$F_{all} = 300 \text{ psi } (2{,}067 \text{ kPa}) \tag{4}$$

This value corresponds to a safety factor of 6.3 based on the average failure stress. The use of such a large safety factor is justified because of the large variability found in the damaged piles. The disadvantage of this method is that many piles would be heavily penalized.

Computation of pile capacity based on net area and clear wood strength

The distribution of failure stress for the 30 piles is erratic and does not follow a specific pattern. However, the failure stresses for the 220 clear wood coupons formed a distribution pattern resembling the normal. The frequency diagram is shown in figure 12 for both piles and coupons where the failure stresses are grouped into 500-psi (3,450 kPa) increments. A statistical analysis (based on ASTM D2915) was conducted to determine an allowable stress for the clear wood samples. ASTM D2915 recommends that the unadjusted allowable stress shall be the five percent exclusion limit (EL) if the percent difference between EL and lower tolerance limit (TL) of the five percent exclusion value is less than five percent. Otherwise the unadjusted allowable stress should be taken as 1.05 TL. A summary of the statistical analysis is

- Mean failure stress = 3,591 psi (24,700 KPa)
- Standard deviation = 1,355 psi (9,340 kPa)

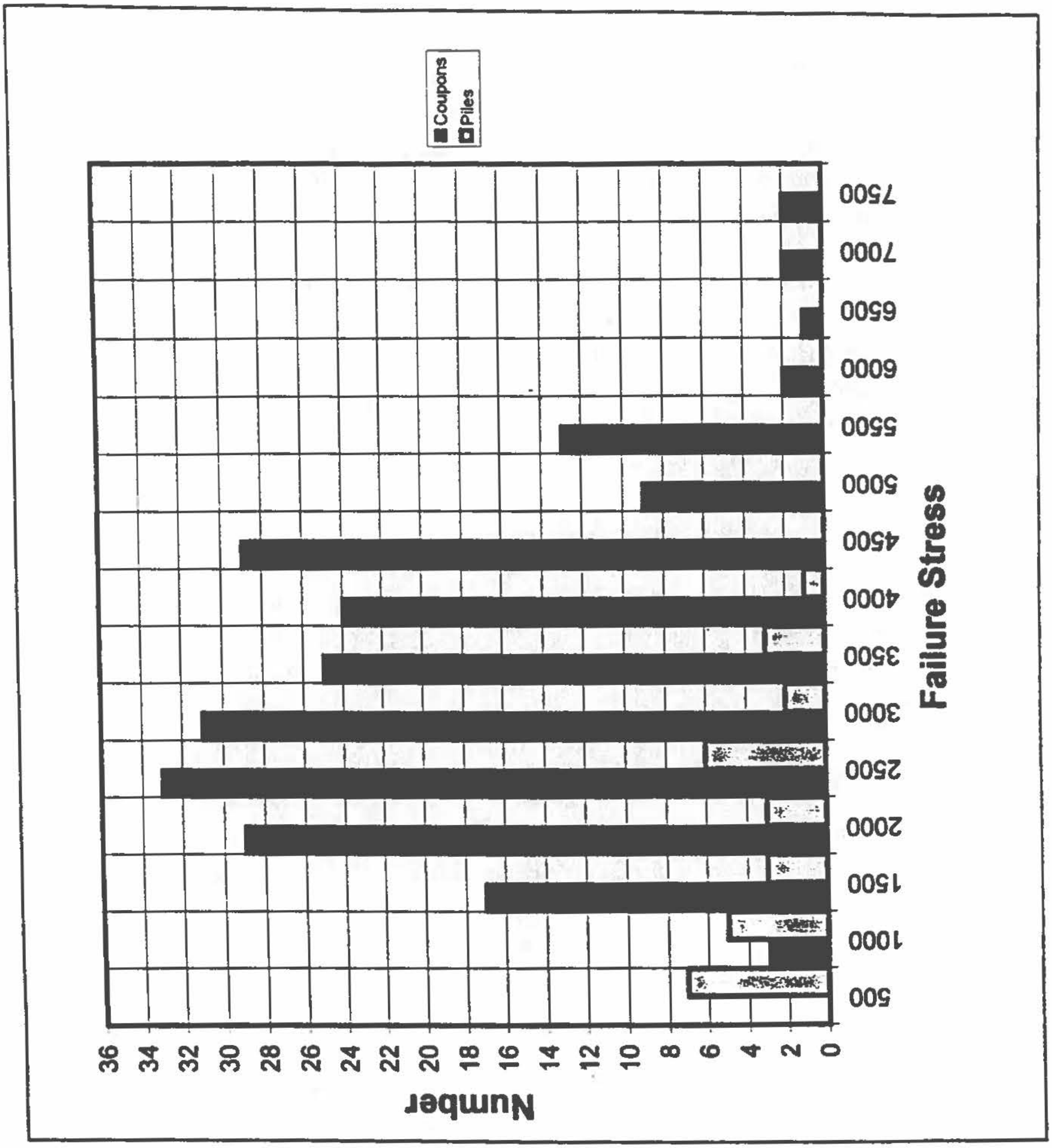

Figure 12
Frequency diagram for both pile and coupon failure stress in 500 psi (3,450 kPa) increments

- 95% confidence interval for the mean = 3,412 to 3,769psi (23,500 to 26,000 kPa)
- 5% exclusion limit, EC = 1,759 psi (12,100 kPa)
- Tolerance limit, TL = 1,609 psi (11,100 kPa)

In this case the 1.05 TL controls and the unadjusted allowable stress is:

$$F^{c}_{all} = 1{,}689 \text{ psi } (11{,}600 \text{ kPa}) \tag{5}$$

However, ASTM D2915 requires a reduction factor of 0.526 for compression parallel-to-grain. Thus, the allowable stress for coupons taken from old solid southern pine piles (rounded to the nearest 25 psi or 50 kPa) is:

$$F^{c}_{all} = 900 \text{ psi } (6{,}150 \text{ kPa}) \tag{6}$$

Comparing this value to the average failure stress, the average safety factor is four. Since a correlation was found between the pile and coupon failure stresses (fig. 11), the pile allowable stress on the net section can be found from the coupon tests. The relationship between the pile failure stress, $\sigma_{p,}$ and the coupon failure stress, σ_c can be written as:

$$\sigma_p = 1.15\ \sigma_c - 2015 \tag{7}$$

where values are in psi.

Since the analysis of the coupon allowable stress resulted in a safety factor of four applied to the mean failure stress, a smaller safety factor can be used for the pile allowable stress. Taking σ_c as four times the allowable coupon stress computed from the samples, the pile allowable stress can be written as:

$$F_{all} = \{1.15\ (4)\ (900) - 2015\}\ /\ 4 = 531 \text{ psi } (3{,}660 \text{ kPa})$$

or rounding down to the nearest 50 psi (or 345 kPa)

$$F_{all} = 500 \text{ psi } (3{,}450 \text{ kPa}) \tag{8}$$

This approach is based on a more statistically justified analysis than equation 4.

Computation of pile capacity based on gross area and effective length

In the first phase of this project an effort was made to determine if a relationship exists between the measured effective length, L_{eff}, and the failure stress. A plot was made for both the stress based on minimum net area (using the smallest net cross section area in the pile) and the stress based on minimum gross area (using the smallest gross cross section area in the pile). While the net stress plot did not yield a significant relationship, the gross stress plot did. The results are shown in figure 13. The piles with an $\ell_{eff} = 0$ failed primarily in crushing. The piles with 10 inches (0.25 m) $\leq \ell_{eff} \leq$ 38 inches (0.97 m) failed in a combination of crushing and some buckling. The piles with $\ell_{eff} >$ 38 inches (0.97 m) failed primarily in shell buckling. The data conforms reasonably well to a classical curve for column behavior: (1) A horizontal line in the crushing zone of small effective lengths, and (2) an Euler buckling curve for longer effective lengths. An approximate curve is plotted in figure 13. The horizontal line is plotted at F_g = 2,000 psi (13,800 kPa) based on A_g which is the two significant figure average of all piles with a measured effective length of less than 38 inches (0.97 m). The approximate Euler elastic buckling curve is based on an average E of 500,000 psi (3,450 MPa) from the results of the pile tests in table 4 and radius of gyration, r = 0.765 inches (19.4 mm). Euler's buckling stress is given as:

$$\sigma_{cr} = \frac{\Pi^2 E r^2}{l_{eff}^2} \tag{9}$$

The significance of the Euler curve can be seen by considering an idealized approximate model for buckling. Assuming that the radial tension stresses are negligible, the hollow pile can be approximated by a series of rectangular shell segments as shown in Figure 14. If each shell segment acts independently during buckling the radius of gyration, r, can be computed as:

$$A = bt \tag{10}$$

$$I = \frac{1}{12} b t^3 \tag{11}$$

$$r^2 = \frac{I}{A} = \frac{t^2}{12} \tag{12}$$

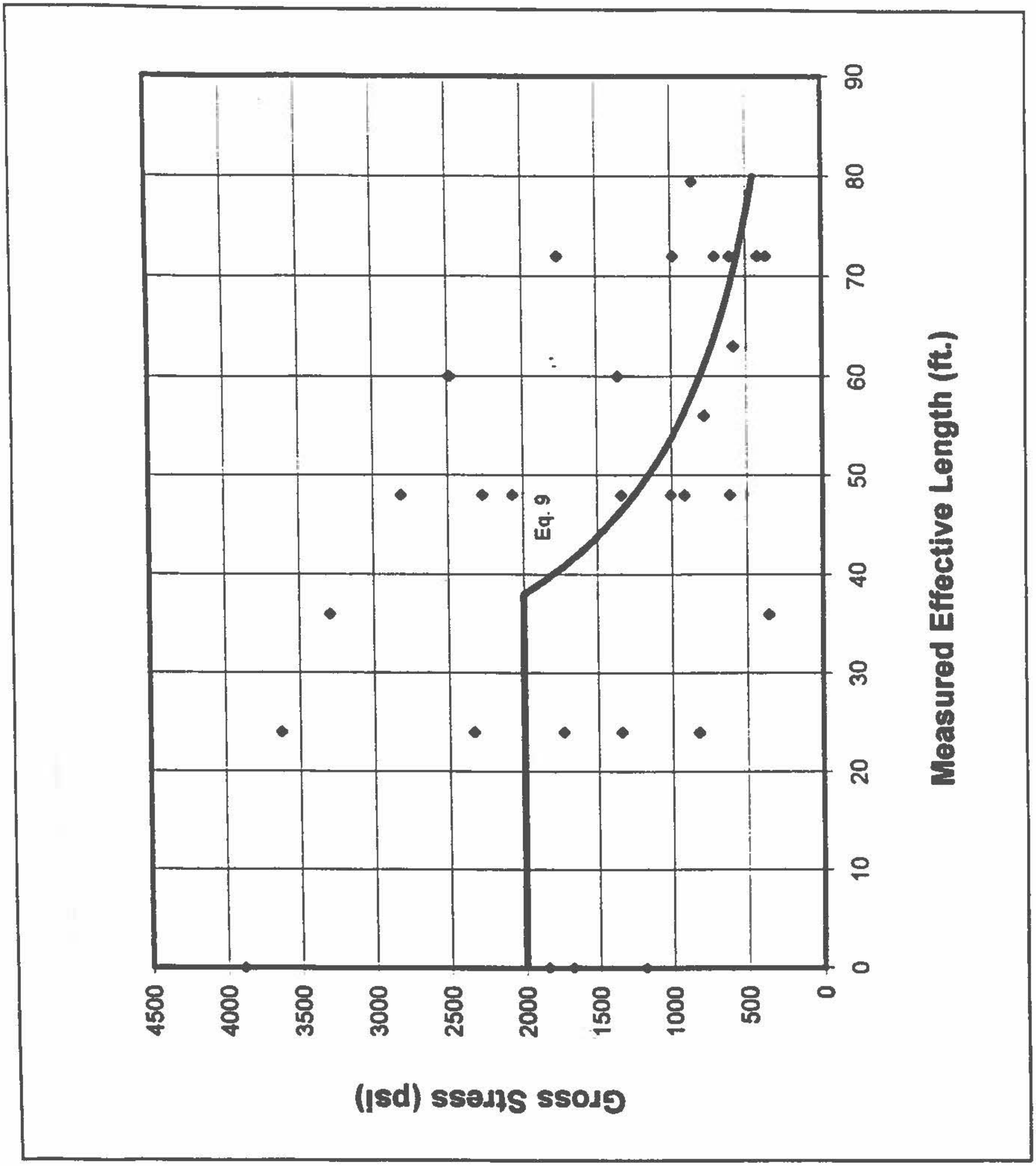

Figure 13
Pile failure stress (based on gross area) versus measured effective length

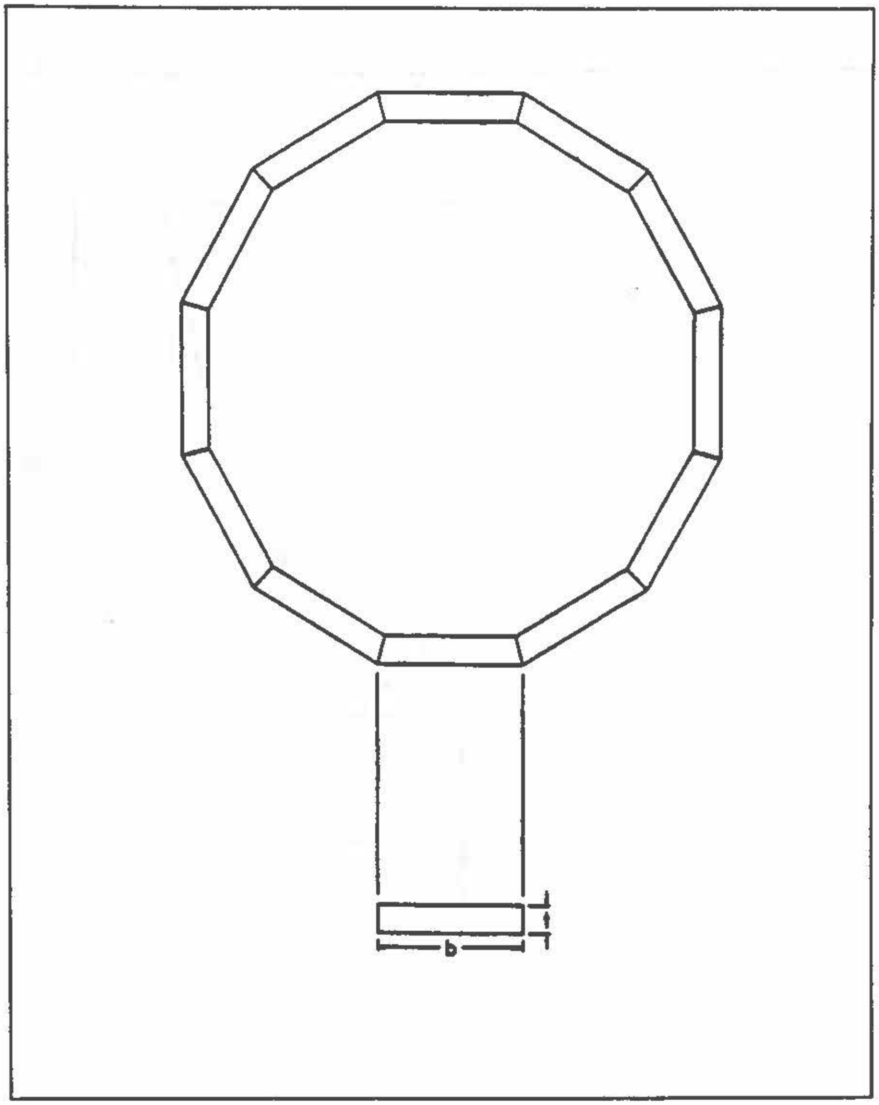

Figure 14
Idealized model for hollow pile buckling

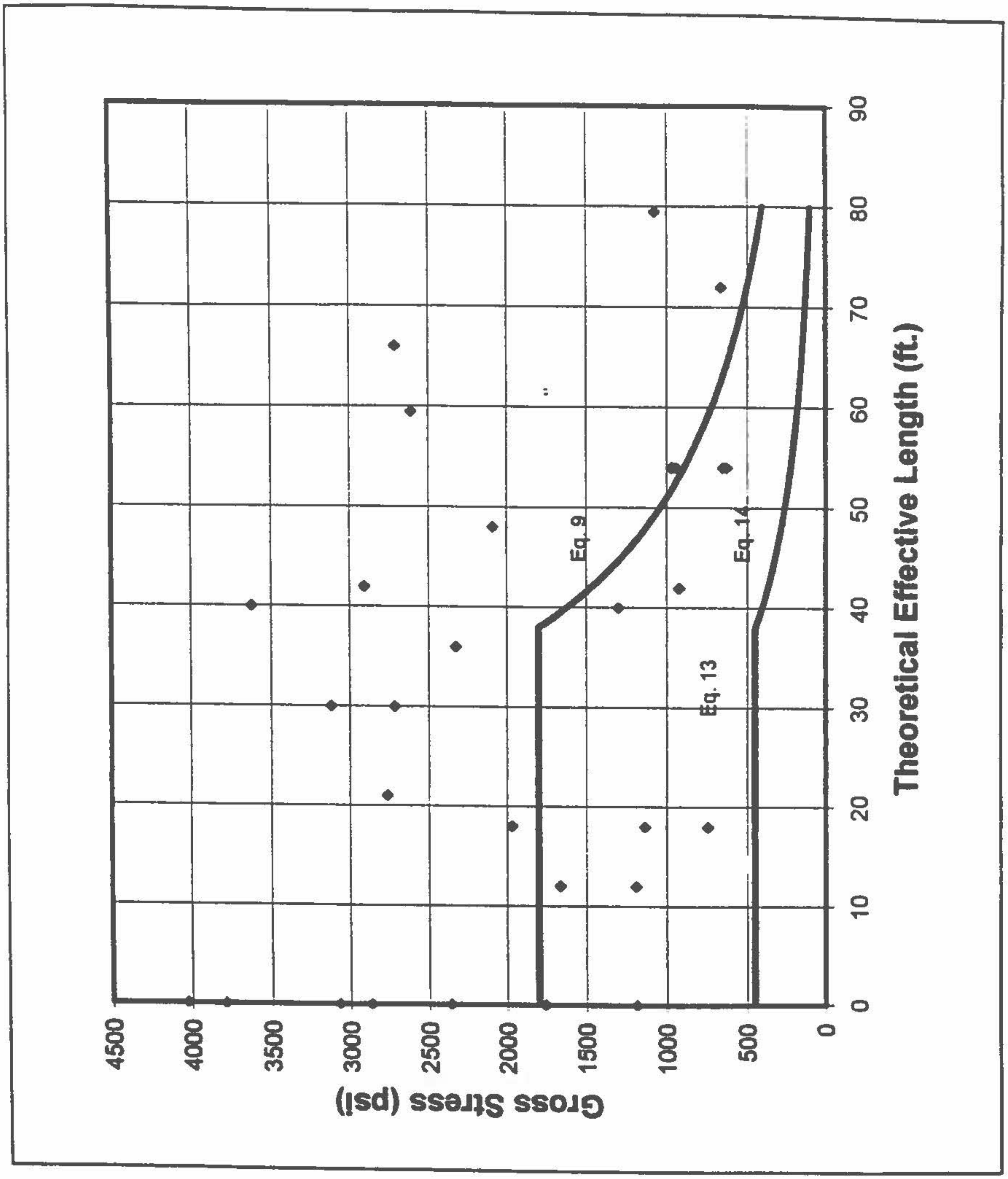

Figure 15
Pile failure stress (based on gross area) versus theoretical effective length

Thus, for the r-value of 0.765 inches (19.4 mm) used in eq. 12, the corresponding shell thickness, t, is equal to 2.65 inches (67.3 mm). This shell thickness is not an unreasonable average based on the hollow cross sections studied. Also, for l_{eff} of 38 inches (965 mm) the Euler's buckling stress is 2,000 psi (13,800 kPa). For this reason, the Euler's curve is used in the model shown in figure 13 for l_{eff} values greater than 38 inches (965 mm).

In order to completely develop a model for pile buckling, a method is needed to determine the theoretical effective length of a hollow cross section. This task is complicated by the fact that the hollow pile cross sections vary dramatically over length, and the void is not necessarily centered at any given cross section. Considering the theoretical shell thickness of approximately three inches (75 mm) computed from the Euler buckling equation 8, an average shell net area would be approximately 80 percent of the gross area.

This procedure can be used for computing the effective length as follows:

1. Plot the A_{net} and A_{gross} over the entire length of the hollow portion of the pile. Such a plot is shown for each hollow pile in appendix I.
2. Plot the value of 80 percent of the minimum A_g over the entire length on the same plot.
3. The effective length is the length over which A_n is less than 80 percent of A_g.

The theoretical values using this method for each pile are given in table 6. The results compare reasonably well to the experimental. A plot of the ultimate stress, F_g, based on gross area, is also plotted with respect to the theoretical effective length in figure 15. For l_{eff} 38 inches (0.965 m), the average A_g is 1,806 psi (12,400 kPa). This value is rounded to 1800 psi (12,400 kPa) and plotted in Fig. 15. An Euler curve is also plotted with E = 500,000 psi (3,450 MPa) and r = 0.726 inches (18.4 mm) which corresponds to an average shell thickness of 2.5 inches (64 mm)

Using a safety factor of four, an allowable stress curve is also shown in figure 15. By this approach, the equations for allowable stress on the gross area are:

For $l_{eff} \leq 38$ in (965 mm):

$$F_{all} = 450 \text{ psi } (3,100 \text{ kPa}) \tag{13}$$

For $\ell_{eff} \geq 38$ in (965 mm):

$$F_{all} = 650{,}000 / (\ell_{eff})^2 \tag{14}$$

where ℓ_{eff} is in inches. It may seem that a model using A_{net} would better account for pile strength. However, the correlation of test results to the combination of A_{net} and ℓ_{eff} was poor. Consequently, A_g was used. However, this method has limited practical application since it is difficult and time consuming to determine the length of the hollow zone. This approach suggests that a lower safety factor of four would be appropriate.

Computation of pile capacity based on coupon failure stress and effective length

Since the capacity of the sound wood varies considerably from pile to pile, the use of the coupon strength should lead to a more accurate prediction of pile capacity. However, it is usually not practical to remove coupons for testing. An alternative is to use a penetration device, which measures the force, required to drive a nail sized probe into the pile for a specified distance. This force can be correlated to the sound wood capacity. Two preliminary series of tests were conducted to investigate this relationship. First, nails (size 8d) were forced into 22 wood coupons taken from the piles. The force at maximum penetration is plotted against coupon failure stress in figure 16. There is a good correlation that can be approximated as:

$$F_{coup} = 100\ F_{nail} \tag{15}$$

Since this portion of the investigation was beyond the project objectives, it was limited in scope. However, the results suggest that a probing device can be developed which will provide an accurate measure of the wood strength.

To further verify that such a relationship exists, nails were pushed into six of the piles. A plot of the penetration energy and the pile net stress (fig. 17) shows a strong correlation given the variability of wood properties.

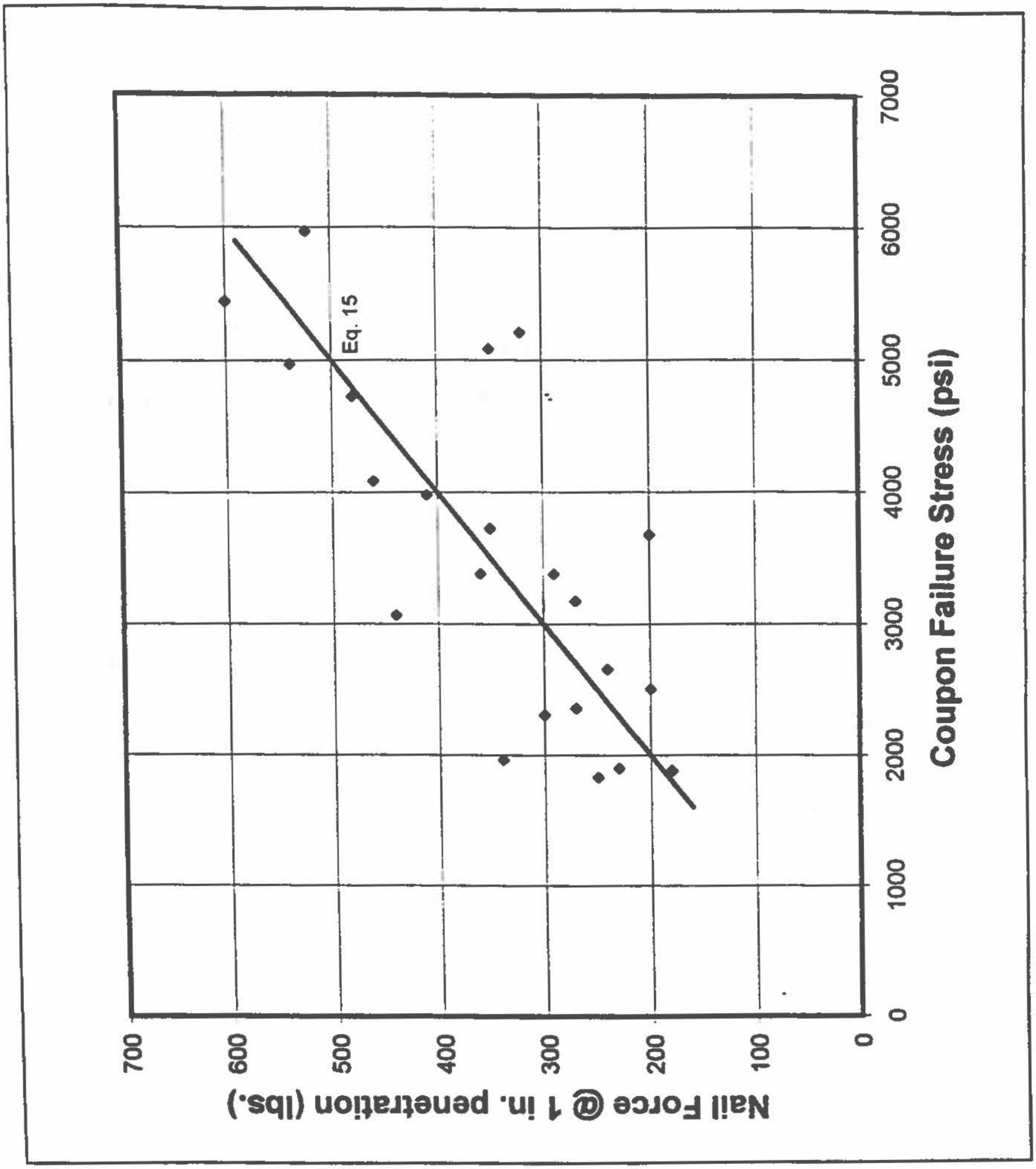

Figure 16
Maximum force required to push an 8 d nail one inch (25 mm) into a coupon versus the coupon compression on failure stress

An approach to predicting pile capacity would be as follows:

1. Use a penetrometer device to obtain the basic wood strength.
2. Compute the effective length of the hollow portion of the pile as previously described.
3. Base the pile capacity on a formula that accounts for both crushing and buckling of the outer shell, depending on the effective length.

To illustrate how this approach would work, the ratio of pile net failure stress and average coupon failure stress was plotted against effective lengths as shown in figure 18. Using l_{eff} = 38 inches (965 mm) as the dividing line between crushing and buckling, an approximate value for the ratio

$$\sigma_{nor} = \sigma_n / \sigma_{coup} \tag{16}$$

is given by

$$\sigma_{nor} = 0.7 \qquad \text{for } l_{eff} \leq 38 \text{ in (965 mm)} \tag{17}$$

$$\sigma_{nor} = 1000 / (\ l_{eff}\ )^2 \qquad \text{for } l_{eff} \geq 38 \text{ in (965 mm)} \tag{18}$$

By normalizing to wood strength, a lower safety factor could be used. For example, a safety factor of three gives

$$F_n = 0.23 \qquad \text{for } \ l_{eff} \leq 38 \text{ in (965 mm} \tag{19}$$

$$F_n = 333 / (l_{eff})^2 \quad \text{for } l_{eff} \geq 38 \text{ in (965 mm):} \tag{20}$$

The approach for computing pile capacity would be:

1. Compute l_{eff} from field measurements as previously described.
2. Calculate F_n from equations 19 and 20.
3. Obtain the penetration data, F_{nail}, from field test of the specific pile.
4. Calculate the wood coupon strength using equation 15.
5. Calculate the pile capacity as $F_{all} = F_n \times F_{coup.}$

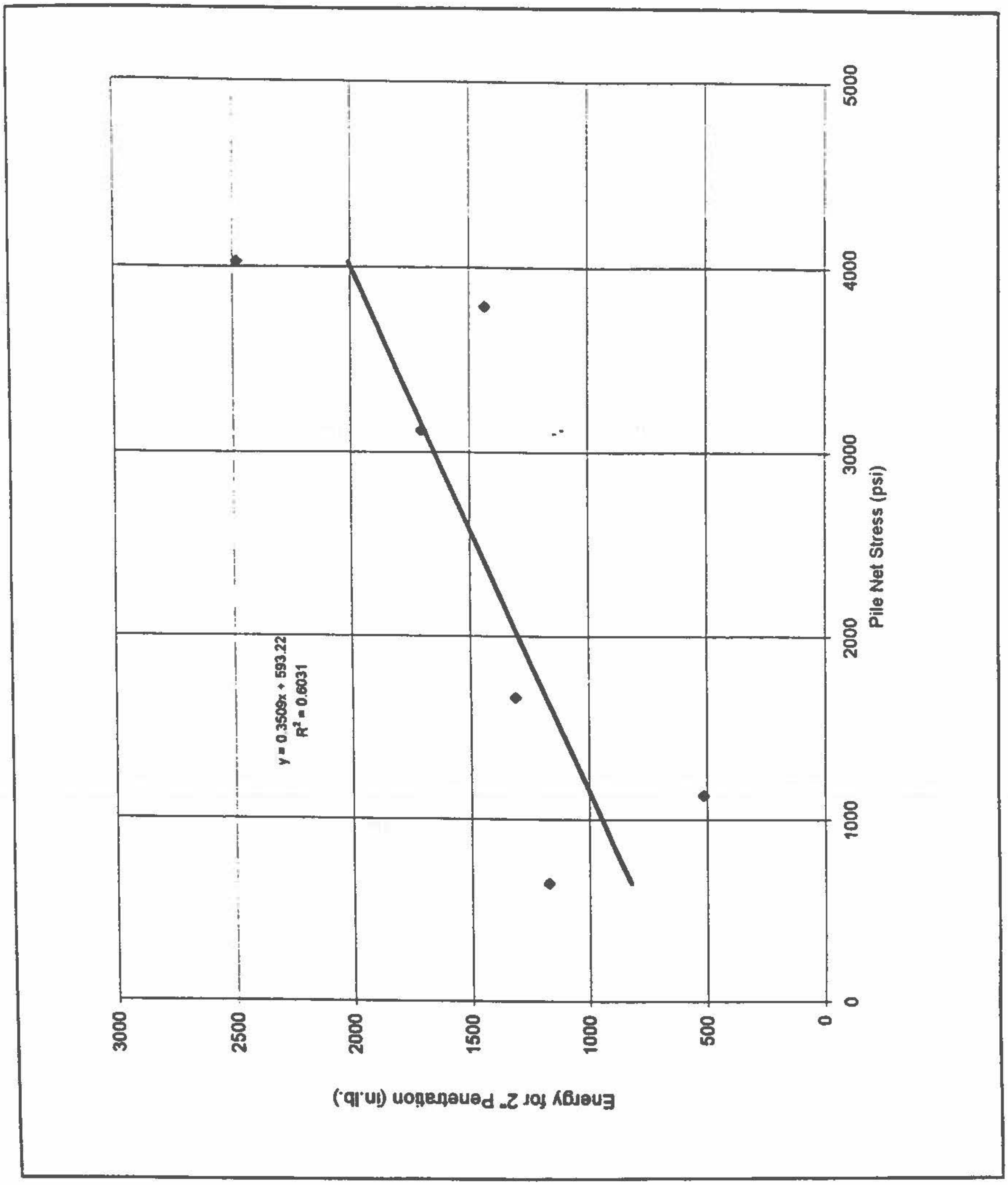

Figure 17
Energy required to push a 20d nail two inches (50 mm) into a timber pile versus the net failure stress of the pile

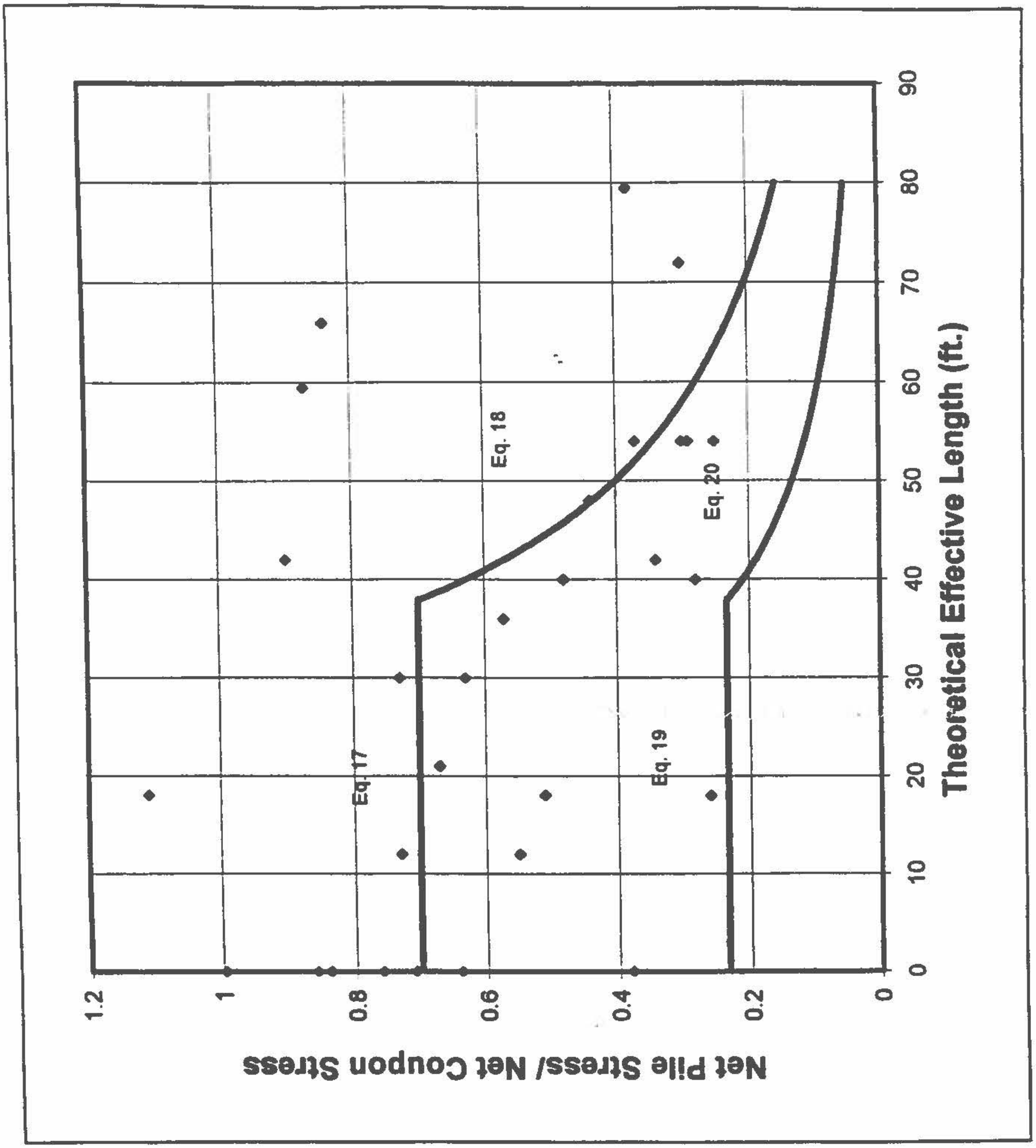

Figure 18
Ratio of pile failure stress (based on net area) and coupon failure stress versus theoretical pile effective length

CONCLUSIONS

The capacity of hollowed timber piles has been investigated both experimentally and theoretically. A series of old decayed piles were removed from in-service bridges for the study. Tests were conducted on both the piles and small coupons taken from the piles. The investigation has led to the following conclusions:

1. The strength of the sound wood portion of decayed piles is significantly lower than that of new piles.

2. Piles having void areas less than approximately 20 percent of the gross area tend to fail primarily by crushing.

3. Piles with void areas greater than 20 percent tend to fail primarily by buckling of the outer shell.

4. A good predictor of the strength of the sound wood in a damaged pile is the nail penetration energy required for a radial penetration to the pile.

5. Using the allowable stress design approach, the allowable capacity of a damaged pile, P_{all}, can be expressed as:

$$P_{all} = F_{all} A_{eff}$$

   where F_{all} is the allowable stress and A_{eff} is the effective area of the pile.

6. A series of approaches for computing F_{all} and A_{eff} were developed. In order of ascending accuracy, the results are:

   a) Based net area and damaged pile test data

   $F_{all} = 300$ psi (2,067 kPa)

   $A_{eff} = A_{net}$ where A_{net} is the minimum area of sound wood

   b) Based on net area and clear wood specimen strength

   $F_{all} = 500$ psi (3,450 kPa)

   $A_{eff} = A_{net}$

   c) Based on gross area and effective length

For $l_{eff} \leq 38$ inches (965 mm)

$F_{all} = 450$ psi (3,100 kPa)

For $l_{eff} \geq 38$ inches (965 mm)

$F_{all} = 650{,}000 / (l_{eff})^2$

$A_{eff} = A_g$

where A_g is the minimum gross area of the pile and l_{eff}

is the pile length over which $A_{net} / A_g = 0.8$

d) Based on clear wood strength and effective length

$F_{all} = F_n F_{coup}$
$A_{eff} = A_{net}$
where
$F_n = 0.23$ for $l_{eff} \leq 38$ inches (965 mm)
$F_n = 333 / (l_{eff})^2$ for $l_{eff} \geq 38$ inches (965 mm)
$F_{coup} = 100 F_{nail}$
F_{nail} = the maximum force generated penetration when uniformly pushing on an 8d nail or similar probe one inch (25 mm) radially into the pile.

The approach using case (d) will provide results most consistent with actual pile strength. However, a pile penetrometer needs to be developed in order to measure clear wood strength without taking coupons for laboratory testing. All cases except (c) require that the net area, A_{net}, be measured or estimated.

RECOMMENDATIONS

1. Development of a pile penetrometer

An accurate analysis of pile capacity depends on knowledge of the clear (or solid) wood strength. Tests have shown that this strength decreases in older piles. The concept of a penetrometer device was developed to access this strength. While the development here was preliminary, good correlation was obtained in the laboratory. What is needed is a field penetrometer, which can be used by bridge inspectors to measure clear wood strength during inspections. This device should be portable (preferably hand-held) with either a manual or automatic pump to force the probe into the pile. The device should have a direct readout, giving clear wood strength.

The development of this device would have broader application than just piles. It could be utilized for evaluating the strength of timber pile caps, beams, and decking.

2. Development of a method is for determining the level of decay for in-service piles.

A second key to predicting the capacity of hollow piles is the measurement of the degree of decay and the minimum net area of the pile. A method is needed for bridge inspectors to rapidly determine this information in the field. The current approach is to use hammer soundings to locate the hollow areas and then drive nails or drill holes to measure the degree of hollowness. An automated procedure would expedite this process. Conceptually, the penetrometer device could also be used to measure the sound wood thickness. This aspect could be incorporated into the penetrometer development.

LIST OF REFERENCES

1. Williams, J. R. and Norton, K. J., "A Decay in Timber Trestles: What is the Rate of Growth?" *Railway and Track Structures*, April 1976, pp. 26-29.

2. Jones, C. P., " Deterioration and Repair of Timber and Concrete Pilings," Florida Cooperative Extension Service, Marine Advisory Program, MAP-27, National Technical Information Service, Springfield, Va., July 1982, pp. 1-14.

3. "For these Wood Piles, Life Begins at 58 Years," *Railway and Track Structures*, Sept. 1973, pp. 27-29.

4. Heising, G. D., "Controlling Wood Deterioration in Waterfront Structures," *Sea Technology*, Vol. 20, No. 6, June 1979, pp.20-21.

5. Freas, A., ed., "Evaluation, Maintenance and Upgrading of Wood Structures," Chapter 5, *Methods of Repair*, ASCE, New York, 1982.

6. "Now: Grout-Filled Timber Piles," *Railway and Track Structures*, Feb. 1973, pp. 28-29.

7. Avent, R. R., "Decay, Weathering and Epoxy Repair of Timber," *Journal of Structural Engineering*, Vol. 111, No.2, ASCE, Feb. 1985, pp. 328-342.

8. "Bridge Pilings Can be Protected; FPR jackets Stop Deterioration," *Better Roads*, May 1980, pp. 20-25.

9. Gerke, R. C., "New Process Restores Timber Piles," *Ocean Industry*, May 1969, pp. 92-93.

10. "Gribbles' Attack Collapses Bridge...But Polyester Sleeves Thwart Them," *Better Roads*, April 1980, pp. 10-14.

11. Rissel, M. C., Graber, D. R., Shoemaker, M. J., and Flournoy, T. S., "Assessment of Deficiencies and Preservation of Bridge Substructures Below the Waterline," NCHRP Report 251, TRB, National Research Council, Washington D. C., Oct. 1982, 79 pp.

12. Fish, A., "Timber Bridges-Inspection Primer," *Railway and Track Structures*, Sept. 1979, pp. 48-49.

13. Anthony, R. W. and Bodig, J., "Nondestructive Evaluation of Timber Structures for Reliable Performance," Proc. 2nd Pacific Timber Engineering Conference, Auckland, New Zealand, 1989.

14. Beall, F. C., and Wilcox, W. W., "Relationship of Acoustic Emission to Mass Loss from Decay during Radial Compressive Testing," Unpublished research note, Weyerhaeuser Company, Tacoma, WA., 1986.

15. Hoyle, R. J. and Pellerin, R. F., "Stress Wave Inspection of a Wood Structures," Proc. 4th Nondestructive Testing of Wood Symp., Washington State University, 1978.

16. Pellerin, R. F., "Inspection of Wood Structures for Decay Using Stress Waves," Proc. 2nd Pacific Timber Engineering Conference, Auckland, New Zealand, 1989.

17. *National Design Specification for Wood Construction*, National Forest and Paper Association, Washington, D. C., 1991.

APPENDIX

Summary of Physical Characteristics for Pile No. 3A

Dimensions								
Section No.	Distance from Top		Circumference		Diameter		Area	
	(m)	(ft.)	(m)	(in.)	(m)	(in.)	(m^2)	(in^2)
1	0.	0	0.97	38.0	0.31.	12.10	0.07	115.0
2	0.31	1	0.95	37.5	0.30	11.94	0.07	112.0
3	0.61	2	0.95	37.5	0.30	11.94	0.07	112.0
4	0.92	3	0.96	37.75	0.31	12.01	0.07	113.3
5	1.22	4	0.97	38.25	0.31	12.18	0.08	116.5

Defects				
Defect No.	Reference Angle (degrees)	Distance from Top		Description
		(m)	(in.)	
1	0	0.20	8	1 in. dia. knot
2	0	0.20	8	small scarf
3	30	0.22	8.5	nail
4	30	0.08	3	nail
5	90	0.99	39	0.875 in. dia. knot
6	135	0.15	6	2" dia. knot and scarf
7	210	0.03	1	nail
8	210	0.15	6	nail
9	210	0.43	17	3 in. scarf
10	275	0.97	38	1 in. dia. knot
11	300	0.23	9	4 0.25 in. dia. hole

Summary of Physical Characteristics for Pile No. 3B

Dimensions

Section No.	Distance from Top		Circumference		Diameter		Area	
	(m)	(ft.)	(m)	(in.)	(m)	(in.)	(m^2)	(in^2)
1	0	0	0.91	36.0	0.29	11.46	0.07	103.1
2	0.31	1	0.93	36.5	0.30	11.62	0.07	106.0
3	0.61	2	0.91	36.0	0.29	11.46	0.07	103.1
4	0.91	3	0.94	37.0	0.30	11.78	0.07	109.0
5	1.22	4	0.98	38.5	0.31	12.25	0.08	117.9

Defects

Defect No.	Reference Angle (degrees)	Distance from Top		Description
		(m)	(in.)	
1	0	0.20	8	small notch
2	0	0.20	8	2" dia. knot
3	30	0.22	8.5	1" dia. knot
4	30	0.08	3	3 x 4" lg. scarf

Summary of Physical Characteristics for Pile No. 4

Dimensions								
Section No.	Distance from Top		Circumference		Diameter		Area	
	(m)	(ft.)	(m)	(in.)	(m)	(in.)	(m^2)	(in^2)
0	0	0	1.04	40.75	0.33	12.97	0.09	132.1
1	0.31	1	1.02	40.25	0.33	12.81	0.08	128.9
2	0.61	2	1.01	39.75	0.32	12.65	0.08	125.7
3	0.91	3	1.00	39.5	0.32	12.57	0.08	124.1
4	1.22	4	1.01	39.6	0.32	12.41	0.08	121.0
5	1.52	5	0.98	38.75	0.31	12.33	0.08	119.4
6	1.83	6	0.97	38.25	0.31	12.18	0.08	116.5
7	2.13	7	0.94	37.0	0.30	11.78	0.07	109.0

Defects				
Defect No.	Reference Angle (degrees)	Distance from Top		Description
		(m)	(in.)	
1	220	1.25	49	Large split 1.25 " @ 1' 2.625" @ 2' 2.75" @ 3' 2.5 @ 4'
2	285	0.25	10	1.375 dia. hole
3	225	0.05	2	1" dia. indentation
4	210	0.43	17	1.75" dia. indentation
5	170	0.13	5	Scarf 3.5" lg. x 1.5" wide
6	135	0.23	9	Split 6.5" lg. x 1.5" wide
7	135	0.37	14.5	1" dia. hole
8	10	1.14	45	1.25" dia. hole

Summary of Physical Characteristics for Pile No. 5

Dimensions								
Section No.	Distance from Top		Circumference		Diameter		Area	
	(m)	(ft.)	(m)	(in.)	(m)	(in.)	(m^2)	(in^2)
0	0	0	0.86	33.75	0.27	10.74	0.06	90.6
1	0.31	1	0.88	34.5	0.28	10.98	0.06	94.7
2	0.61	2	0.91	36.0	0.29	11.46	0.07	103.1
3	0.91	3	0.90	35.25	0.29	11.22	0.06	98.9
4	1.22	4	0.91	35.75	0.29	11.38	0.07	101.7
5	1.52	5	0.90	35.5	0.29	11.3	0.07	100.3

Defects				
Defect No.	Reference Angle (degrees)	Distance from Top		Description
		(m)	(in.)	
1	0	0.33	13	4.5" dia. knot
2	45	0.11	4.5	3/4" dia. hole
3	45	0.38	15	1 ½" wide split
4	45	1.35	53	7" long 4" wide scarf
5	120	0.22	8.5	5/8" dia. hole
6	135	0.45	17.5	1" dia. knot
7	180	0.61	24	1.5" dia. knot
8	220	0.91	36	24" lg. x 2.75" wide split
9	230	0.11	4.5	1" dia. hole
10	230	0.69	27	0.75" dia. hole
11	230	1.22	48	1.5" dia. hole
12	250	1.22	48	2" dia. knot
13	270	1.52	60	1.5" dia. knot
14	340	0.47	18.5	3" dia. knot

Summary of Physical Characteristics for Pile No. 6

Dimensions								
Section No.	Distance from Top		Circumference		Diameter		Area	
	(m)	(ft.)	(m)	(in.)	(m)	(in.)	(m^2)	(in^2)
0	0	0	1.12	44.25	0.36	14.09	0.10	155.9
1	0.31	1	1.13	44.5	0.36	14.16	0.10	157.5
2	0.61	2	1.11	43.5	0.35	13.85	0.10	150.7
3	0.91	3	1.10	43.25	0.35	13.77	0.10	148.9
4	1.22	4	1.08	42.35	0.34	13.45	0.09	142.1
5	18.14	59.5"	1.06	41.75	0.34	13.29	0.09	138.7

Defects				
Defect No.	Reference Angle (degrees)	Distance from Top		Description
		(m)	(in.)	
1	75	0.83	32.5	4.5" lg. x 4" wide scarf
2	100	0.61	24	1" dia. knot
3	100	0.99	39	nail
4	275	0.64	25	1" dia. knot
5	280	0.55	21.5	0.5" hole
6	300	1.22	48	11" lg. x 1" wide x 0.75 deep scarf
7	340	0	0	6" lg. x 1" wide scarf
8	90	1.02	40	0.75" dia. hole
9	90	1.47	58	0.75" dia. hole
10	100	1.42	56	1" dia. hole

Checking throughout with max. width of 3/8".

Summary of Physical Characteristics for Pile No. 7

Dimensions

Section No.	Distance from Top		Circumference		Diameter		Area	
	(m)	(ft.)	(m)	(in.)	(m)	(in.)	(m^2)	(in^2)
0	0	0	0.946	37.25	0.301	11.86	0.071	110.5
1	0.305	1	0.978	38.5	0.311	12.25	0.076	117.9
2	0.610	2	0.978	38.5	0.311	12.25	0.076	117.9
3	0.914	3	0.965	38.0	0.307	12.10	0.074	115.0
4	1.219	4	0.965	38.0	0.307	12.10	0.074	115.0
5	1.524	5	1.003	39.5	0.319	12.57	0.080	124.1
6	1.829	6	0.991	39.0	0.315	12.41	0.078	121.0

Defects

Defect No.	Reference Angle (degrees)	Distance from Top		Description
		(m)	(in.)	
1	315	0.203	8	2" dia. knot
2	0	0.965	38	3.5" dia. knot
3	0	1.753	69	2" dia. knot
4	315	1.486	58.5	2" dia. knot
5	90	0.203	8	1.75" dia. knot
6	130	0.787	31	1.25" dia. knot
7	135	1.041	41	1.5" dia. knot
8	135	1.334	52.5	1.5" dia. knot
9	220	0.813	32	1.5" dia. knot
10	90	0	0	Notch @ 7.5" lg. x 1.5" wide x 5/8" deep
11	130	0.914	36	5/8" dia. hole, 1.25" deep
12	140	0.686	27	5.8" dia. hole, 2.25" deep
13	180	1.029	40.5	Notch 3.25" wide x 0.5" deep
14	225	0	0	Notch entire length - 2.25" wide @ top and 2" wide @ bottom
15	10	0.711	28	Nail
16	10	0.089	3.5	Nail
17	200	0.762	30	3 nails

Summary of Physical Characteristics for Pile No. 8A

Dimensions

Section No.	Distance from Top		Circumference		Diameter		Area	
	(m)	(ft.)	(m)	(in.)	(m)	(in.)	(m^2)	(in^2)
1	0	0	0.972	38.25	0.309	12.18	0.752	116.5
2	0.305	1	0.997	39.25	0.317	12.49	0.790	122.5
3	0.610	2	0.997	39.25	0.317	12.49	0.790	122.5
4	0.914	3	1.010	39.75	0.321	12.65	0.811	125.7
5	1.219	4	1.041	41.0	0.331	13.05	0.863	133.8
6	1.524	5	1.041	41.0	0.331	13.05	0.863	133.8
7	1.829	6	1.067	42.0	0.340	13.37	0.906	140.4
8	2.019	6.625	1.073	42.25	0.342	13.45	0.917	142.1

Defects

Defect No.	Reference Angle (degrees)	Distance from Top		Description
		(m)	(in.)	
1	270	0.838	33	12" lg. x 5/8" wide scarf
2	45	0.406	16	0.75" dia. hole
3	45	1.372	54	1 3/8" dia. hole
4	40	1.524	60	6" lg. x ½" wide scarf
5	225	0	0	2 splits - 5' lg., ½ wide max.

Summary of Physical Characteristics for Pile No. 8B

Dimensions								
Section No.	Distance from Top		Circumference		Diameter		Area	
	(m)	(ft.)	(m)	(in.)	(m)	(in.)	(m^2)	(in^2)
0	0	0	0.959	37.75	0.305	12.02	0.732	113.5
1	0.305	1	0.978	38.5	0.311	12.25	0.761	117.9
2	0.610	2	0.984	38.75	0.313	12.33	0.770	119.4
3	0.680	2.23	0.972	38.25	0.309	12.18	0.752	116.5

Defects				
Defect No.	Reference Angle (degrees)	Distance from Top		Description
		(m)	(in.)	
1	45	0	0	Large split - 3/4" wide

Summary of Physical Characteristics for Pile No. 9

Dimensions

Section No.	Distance from Top		Circumference		Diameter		Area	
	(m)	(ft.)	(m)	(in.)	(m)	(in.)	(m^2)	(in^2)
0	0	0	0.991	39.0	0.315	12.41	0.781	121.0
1	0.305	1	1.003	39.5	0.319	12.57	0.801	124.1
2	0.610	2	1.022	40.25	0.325	12.81	0.832	128.9
3	0.914	3	1.029	40.5	0.327	12.89	0.842	130.5
4	1.219	4	1.054	41.5	0.335	13.2	0.883	136.8
5	1.396	4.58	1.054	41.5	0.335	13.2	0.883	136.8

Defects

Defect No.	Reference Angle (degrees)	Distance from Top		Description
		(m)	(in.)	
				Solid pile - no defects

Summary of Physical Characteristics for Pile No. 10

Dimensions								
Section No.	Distance from Top		Circumference		Diameter		Area	
	(m)	(ft.)	(m)	(in.)	(m)	(in.)	(m^2)	(in^2)
1	0	0	0.956	37.63	0.304	11.97	0.726	112.5
2	0.305	1	0.965	38.0	0.307	12.10	0.742	115.0
3	0.610	2	0.962	37.88	0.306	12.05	0.735	114.0
4	0.914	3	1.045	41.13	0.333	13.10	0.870	134.8
5	1.219	4	1.026	40.38	0.326	12.85	0.837	129.7

Defects				
Defect No.	Reference Angle (degrees)	Distance from Top		Description
		(m)	(in.)	
1	0	0.864	34.0	1 3/4" knot
2	45	0.610	24.0	1/4" split
3	45	0.832	32.75	1 ½" knot
4	175	0.254	10.0	28" lg. x 2 3/4" wide scarf
5	190	-0.838	0-33"	1/4" wide split
6	270	0	0	1/4" wide split
7	315	0.305	12	Missing section - 2" wide, 1 1/4" deep

Summary of Physical Characteristics for Pile No. 11

Dimensions

Section No.	Distance from Top		Circumference		Diameter		Area	
	(m)	(ft.)	(m)	(in.)	(m)	(in.)	(m^2)	(in^2)
1	0	0	0.959	37.75	0.305	12.01	0.731	113.3
2	0.305	1	0.959	37.75	0.305	12.01	0.731	113.3
3	0.610	2	0.965	38.0	0.307	12.10	0.742	115.0
4	0.914	3	0.965	38.0	0.307	12.10	0.742	115.0
5	1.219	4	0.997	39.25	0.318	12.50	0.792	122.7
6	1.524	5	0.997	39.25	0.319	12.57	0.803	124.1

Defects

Defect No.	Reference Angle (degrees)	Distance from Top		Description
		(m)	(in.)	
1	30	0	0	Split 20" long; width 2" @ top
2	90	0.279	11	9" lg. x 2" wide scarf
3	200	-0.610	0-24	Crack 24" lg. x 1/8" wide
4	310	-0.737	0-29	3/16" wide crack
5				Random checking; 1/16" max. width

Summary of Physical Characteristics for Pile No. 12

Dimensions

Section No.	Distance from Top		Circumference		Diameter		Area	
	(m)	(ft.)	(m)	(in.)	(m)	(in.)	(m^2)	(in^2)
1	0	0	1.000	39.38	0.318	12.53	0.795	123.3
2	0.305	1	0.994	39.13	0.316	12.45	0.785	121.7
3	0.610	2	0.997	39.25	0.318	12.5	0.792	122.7
4	0.914	3	0.994	39.13	0.316	12.45	0.785	121.7
5	1.219	4	1.000	39.38	0.318	12.53	0.795	123.3
6	1.524	5	1.010	39.75	0.321	12.65	0.811	125.7
7	1.829	6	1.022	40.25	0.325	12.81	0.832	128.9
8	2.134	7	1.038	40.88	0.330	13.01	0.857	132.9

Defects

Defect No.	Reference Angle (degrees)	Distance from Top		Description
		(m)	(in.)	
1	0	1.473	58.0	1/4" dia. hole
2	0	1.524	60.0	1/4" dia. hole
3	0	1.791	70.5	1/4" dia. hole
4	0	2.083	82.0	7/8" dia. hole
5	90	0.686	27.0	38" long scarf
6	345	0	0	25" lg. x ½" wide @ top of crack
7				Random checking - 1/8" max. width

Summary of Physical Characteristics for Pile No. 13

Dimensions								
Section No.	Distance from Top		Circumference		Diameter		Area	
	(m)	(ft.)	(m)	(in.)	(m)	(in.)	(m^2)	(in^2)
1	0	0	1.022	40.25	0.325	12.81	0.832	128.9
2	0.305	1	1.013	39.88	0.322	12.69	0.816	126.5
3	0.610	2	1.003	39.5	0.319	12.57	0.801	124.1
4	0.914	3	0.994	39.13	0.316	12.45	0.785	121.7
5	1.219	4	0.991	39.0	0.315	12.41	0.781	121.0
6	1.524	5	0.978	38.5	0.311	12.25	0.761	117.9
7	1.829	6	0.972	38.25	0.309	12.17	0.750	116.3
8	2.128	6.98	0.969	38.13	0.308	12.13	0.74	115.6

Defects				
Defect No.	Reference Angle (degrees)	Distance from Top		Description
		(m)	(in.)	
1	0	0.762	30.0	1" dia. gauge; 3/8" deep
2	80	1.041	41.0	1/4" dia. hole
3	80	1.118	44.0	1" dia. hole
4	270	0.762	30.0	5" lg. x 2" wide hole
5	270	0.9525	37.5	½" dia. hole; 5" deep
6	270	1.067	42.0	36" long, max. width of 3.5, 4.5" deep missing section

Summary of Physical Characteristics for Pile No. 14

Dimensions								
Sect. No.	**Distance from Top**		**Circumference**		**Diameter**		**Area**	
	(m)	(ft.)	(m)	(in.)	(m)	(in.)	(m^2)	(in^2)
0	0.000	0	0.972	38.25	0.309	12.18	0.075	116.43
1	0.305	1	0.965	38.00	0.307	12.10	0.074	114.91
2	0.610	2	0.940	37.00	0.299	11.78	0.070	108.94
3	0.914	3	0.940	37.00	0.299	11.78	0.070	108.94
4	1.219	4	0.953	37.50	0.303	11.94	0.072	111.91
5	1.524	5	0.953	37.50	0.303	11.94	0.072	111.91

Defects				
Defect No.	**Reference Angle**	**Distance from Top**		**Description**
	(degrees)	(m)	(in.)	
1	350	0.330	13	2" dia. knot
2	90	1.080	42.5	3.5" dia. knot
3	90	0.305	12	4.5" dia. knot
4	85	0.559	22	Nailhole

Summary of Physical Characteristics for Pile No. 15

Dimensions								
Sect.	Distance from Top		Circumference		Diameter		Area	
No.	(m)	(ft.)	(m)	(in.)	(m)	(in.)	(m^2)	(in^2)
0	0.000	0	0.946	37.25	0.301	11.86	0.071	110.42
1	0.305	1	0.953	37.50	0.303	11.94	0.072	111.91
2	0.610	2	0.978	38.50	0.311	12.26	0.076	117.95
3	0.914	3	0.978	38.50	0.311	12.26	0.076	117.95
4	1.219	4	0.965	38.00	0.307	12.10	0.074	114.91
5	1.524	5	0.994	39.13	0.316	12.45	0.079	121.82

Defects				
Defect	Reference Angle	Distance from Top		Description
No.	(degrees)	(m)	(in.)	
1	80	0.356	14	4" dia. knot
2	135	0.686	27	3.5" dia. knot
3	45	0.635	25	3" dia. knot
4	330	0.559	22	7" dia. knot
5	175	0.864	34	2.5" dia. knot
6	45	1.473	58	2" dia. knot

Summary of Physical Characteristics for Pile No. 16

Dimensions								
Sect.	Distance from Top		Circumference		Diameter		Area	
No.	(m)	(ft.)	(m)	(in.)	(m)	(in.)	(m^2)	(in^2)
0	0.000	0	0.994	39.13	0.316	12.45	0.079	121.82
1	0.305	1	0.978	38.50	0.311	12.26	0.076	117.95
2	0.610	2	0.978	38.50	0.311	12.26	0.076	117.95
3	0.914	3	0.978	38.50	0.311	12.26	0.076	117.95
4	1.219	4	0.978	38.50	0.311	12.26	0.076	117.95
5	1.524	5	0.978	38.50	0.311	12.26	0.076	117.95

Defects				
Defect	Reference Angle	Distance from Top		Description
No.	(degrees)	(m)	(in.)	
1	195	0.127	5	Nailhole
2	180	0.127	5	Nailhole
3	190	0.127	5	Nailhole
4	165	0.356	14	Scar 2.5" long X 1" wide
5	300	0.813	32	4"dia. knot
6	300	1.067	42	4" dia. knot
7	65	1.041	41	2" dia. knot

Summary of Physical Characteristics for Pile No. 17

Dimensions								
Sect. No.	Distance from Top		Circumference		Diameter		Area	
	(m)	(ft.)	(m)	(in.)	(m)	(in.)	(m^2)	(in^2)
0	0.000	0	0.991	39.00	0.315	12.41	0.078	121.04
1	0.305	1	0.978	38.50	0.311	12.26	0.076	117.95
2	0.610	2	0.978	38.50	0.311	12.26	0.076	117.95
3	0.914	3	0.978	38.50	0.311	12.26	0.076	117.95
4	1.219	4	0.978	38.50	0.311	12.26	0.076	117.95
5	1.524	5	0.991	39.00	0.315	12.41	0.078	121.04

Defects				
Defect No.	Reference Angle	Distance from Top		Description
	(degrees)	(m)	(in.)	
1	315	0.000	0	Split 18" long
2	190	0.000	0	Split 2" long
3	165	0.610	24	Nailhole
4	135	0.584	23	Nailhole
5	130	0.203	8	Scarf 2" X 12" X .25" deep

Summary of Physical Characteristics for Pile No. 18

Dimensions								
Sect. No.	Distance from Top		Circumference		Diameter		Area	
	(m)	(ft.)	(m)	(in.)	(m)	(in.)	(m^2)	(in^2)
0	0.000	0	0.946	37.25	0.301	11.86	0.071	110.42
1	0.305	1	0.946	37.25	0.301	11.86	0.071	110.42
2	0.610	2	0.940	37.00	0.299	11.78	0.070	108.94
3	0.914	3	0.933	36.75	0.297	11.70	0.069	107.48
4	1.219	4	0.927	36.50	0.295	11.62	0.068	106.02
5	1.524	5	0.940	37.00	0.299	11.78	0.070	108.94

Defects				
Defect No.	Reference Angle	Distance from Top		Description
	(degrees)	(m)	(in.)	
1	345	0.889	35	Scarf 1" X 2" X .25" deep
2	195	1.067	42	Gash 2" X 5" X .5" deep
3	60	1.092	43	Gash 1.5" X 5" X .25" deep
4	15	0.445	17.5	Nailhole

Summary of Physical Characteristics for Pile No. 19

Dimensions								
Sect.	Distance from Top		Circumference		Diameter		Area	
No.	(m)	(ft.)	(m)	(in.)	(m)	(in.)	(m^2)	(in^2)
0	0.000	0	0.940	37.00	0.299	11.78	0.070	108.94
1	0.305	1	0.953	37.50	0.303	11.94	0.072	111.91
2	0.610	2	0.953	37.50	0.303	11.94	0.072	111.91
3	0.914	3	0.956	37.63	0.304	11.98	0.073	112.65
4	1.219	4	0.965	38.00	0.307	12.10	0.074	114.91
5	1.524	5	0.965	38.00	0.307	12.10	0.074	114.91
6	1.829	6	0.975	38.38	0.310	12.22	0.076	117.19

Defects				
Defect	Reference Angle	Distance from Top		Description
No.	(degrees)	(m)	(in.)	
1	115	1.041	41	Nailhole

Summary of Physical Characteristics for Pile No. 20

Dimensions								
Sect. No.	Distance from Top		Circumference		Diameter		Area	
	(m)	(ft.)	(m)	(in.)	(m)	(in.)	(m^2)	(in^2)
0	0.000	0	1.010	39.75	0.321	12.65	0.081	125.74
1	0.305	1	1.010	39.75	0.321	12.65	0.081	125.74
2	0.610	2	1.019	40.13	0.324	12.77	0.083	128.12
3	0.914	3	1.000	39.38	0.318	12.53	0.080	123.38
4	1.219	4	1.000	39.38	0.318	12.53	0.080	123.38
5	1.524	5	1.000	39.38	0.318	12.53	0.080	123.38
6	1.829	6	0.991	39.00	0.315	12.41	0.078	121.04

Defects				
Defect No.	Reference Angle	Distance from Top		Description
	(degrees)	(m)	(in.)	
1	345	0.203	8	Nailhole
2	260	0.140	5.5	Nailhole
3	260	0.152	6	Nailhole
4	260	0.000	0	Split 19" long
5	250	1.130	44.5	Nailhole
6	40	0.000	0	Split 6" long

Summary of Physical Characteristics for Pile No. 21

Dimensions								
Sect. No.	Distance from Top		Circumference		Diameter		Area	
	(m)	(ft.)	(m)	(in.)	(m)	(in.)	(m^2)	(in^2)
0	0.000	0	0.953	37.50	0.303	11.94	0.072	111.91
1	0.305	1	0.972	38.25	0.309	12.18	0.075	116.43
2	1.219	4	0.965	38.00	0.307	12.10	0.074	114.91
3	1.524	5	0.953	37.50	0.303	11.94	0.072	111.91
4	1.829	6	0.953	37.50	0.303	11.94	0.072	111.91

Defects				
Defect No.	Reference Angle	Distance from Top		Description
	(degrees)	(m)	(in.)	
1	85	0.000	0	Scarf 14" X 1" X 1.25" deep
2	240	0.000	0	Scarf 19" X 4" X 1.2" deep

Summary of Physical Characteristics for Pile No. 23

Dimensions								
Sect. No.	Distance from Top (m)	Distance from Top (ft.)	Circumference (m)	Circumference (in.)	Diameter (m)	Diameter (in.)	Area (m^2)	Area (in^2)
0	0.000	0	1.118	44.00	0.356	14.01	0.099	154.06
1	0.305	1	1.143	45.00	0.364	14.32	0.104	161.15
2	0.610	2	1.168	46.00	0.372	14.64	0.109	168.39
3	0.914	3	1.181	46.50	0.376	14.80	0.111	172.07
4	1.219	4	1.207	47.50	0.384	15.12	0.116	179.55
5	1.524	5	1.241	48.88	0.395	15.56	0.123	190.09
6	1.829	6	1.270	50.00	0.404	15.92	0.128	198.95

Defects				
Defect No.	Reference Angle (degrees)	Distance from Top (m)	Distance from Top (in.)	Description
1	0	0.660	26	Nailhole
2	5	0.737	29	Nailhole
3	5	0.635	25	Nailhole
4	110	0.038	1.5	1" dia. hole
5	290	0.038	1.5	1" dia. hole
6	200	0.533	21	.5" dia. hole
7	255	0.000	0	Decay 7" wide X 50" long
8	255	0.533	21	Elliptical hole 11" X 3.5"
9	290	1.778	70	1" dia. hole
10	90	1.778	70	1" dia. hole

Summary of Physical Characteristics for Pile No. 24

Dimensions								
Sect.	Distance from Top		Circumference		Diameter		Area	
No.	(m)	(ft.)	(m)	(in.)	(m)	(in.)	(m^2)	(in^2)
0	0.000	0	0.946	37.25	0.301	11.86	0.071	110.42
1	0.305	1	0.953	37.50	0.303	11.94	0.072	111.91
2	0.610	2	0.953	37.50	0.303	11.94	0.072	111.91
3	0.914	3	0.946	37.25	0.301	11.86	0.071	110.42
4	1.219	4	0.975	38.38	0.310	12.22	0.076	117.19
5	1.524	5	1.010	39.75	0.321	12.65	0.081	125.74
6	1.829	6	1.029	40.50	0.327	12.89	0.084	130.53

Defects				
Defect	Reference Angle	Distance from Top		Description
No.	(degrees)	(m)	(in.)	
1	80	0.127	5	2" dia. knot
2	130	0.165	6.5	2.5" dia. knot
3	165	0.165	6.5	.5" dia. hole
4	300	0.165	6.5	.5" dia. hole
5	355	0.140	5.5	1.5 " dia. knot
6	300	0.813	32	Split to bottom
7	300	0.711	28	Scarf 27" X 6" X 2.5" deep
8	300	0.838	33	1" dia. hole 11" long

Summary of Physical Characteristics for Pile No. 25

Dimensions								
Sect. No.	Distance from Top		Circumference		Diameter		Area	
	(m)	(ft.)	(m)	(in.)	(m)	(in.)	(m^2)	(in^2)
0	0.000	0	0.981	38.63	0.312	12.29	0.077	118.72
1	0.305	1	0.978	38.50	0.311	12.26	0.076	117.95
2	0.610	2	0.984	38.75	0.313	12.33	0.077	119.49
3	0.914	3	0.978	38.50	0.311	12.26	0.076	117.95
4	1.219	4	0.959	37.75	0.305	12.02	0.073	113.40

Defects				
Defect No.	Reference Angle	Distance from Top		Description
	(degrees)	(m)	(in.)	
1	150	0.152	6	Nailhole
2	255	0.229	9	Nailhole
3	145	0.229	9	Nailhole

Summary of Physical Characteristics for Pile No. 26

Dimensions								
Sect.	**Distance from Top**		**Circumference**		**Diameter**		**Area**	
No.	(m)	(ft.)	(m)	(in.)	(m)	(in.)	(m^2)	(in^2)
0	0.000	0	1.041	41.00	0.331	13.05	0.086	133.77
1	0.305	1	1.029	40.50	0.327	12.89	0.084	130.53
2	0.610	2	1.080	42.50	0.344	13.53	0.093	143.74
3	0.914	3	1.108	43.63	0.353	13.89	0.098	151.45
4	1.219	4	1.137	44.75	0.362	14.24	0.103	159.36
5	1.524	5	1.178	46.38	0.375	14.76	0.110	171.14
6	1.829	6	1.213	47.75	0.386	15.20	0.117	181.44

Defects				
Defect	**Reference Angle**	**Distance from Top**		**Description**
No.	(degrees)	(m)	(in.)	
1	95	1.651	65	1" dia. hole
2	245 - 345	0.000	0	Scarf 24" X 1" deep
3	90 - 180	0.000	0	Scarf 28" X 1" deep
4	275	1.651	65	1" dia. hole

Summary of Physical Characteristics for Pile No. 27

Dimensions								
Sect. No.	Distance from Top		Circumference		Diameter		Area	
	(m)	(ft.)	(m)	(in.)	(m)	(in.)	(m^2)	(in^2)
0	0.000	0	0.991	39.00	0.315	12.41	0.078	121.04
1	0.305	1	0.991	39.00	0.315	12.41	0.078	121.04
2	0.610	2	1.054	41.50	0.336	13.21	0.088	137.05
3	0.914	3	1.086	42.75	0.346	13.61	0.094	145.43
4	1.219	4	1.118	44.00	0.356	14.01	0.099	154.06
5	1.524	5	1.149	45.25	0.366	14.40	0.105	162.94
6	1.829	6	1.184	46.63	0.377	14.84	0.112	172.99

Defects				
Defect No.	Reference Angle	Distance from Top		Description
	(degrees)	(m)	(in.)	
1	0 - 360	0.483	19	Increasing circumference (39" ->45")
2	260	0.559	22	Hole 4" X .5"
3	90	1.194	47	Hole 4" X 1"
4	25	1.676	66	1.5" dia. hole
5	205	1.676	66	1.5" dia. hole
6	260	1.575	62	Hole 10" X 3.5"

Summary of Physical Characteristics for Pile No. 28

Dimensions								
Sect. No.	Distance from Top		Circumference		Diameter		Area	
	(m)	(ft.)	(m)	(in.)	(m)	(in.)	(m^2)	(in^2)
0	0.000	0	0.883	34.75	0.281	11.06	0.062	96.10
1	0.305	1	0.927	36.50	0.295	11.62	0.068	106.02
2	0.610	2	1.035	40.75	0.329	12.97	0.085	132.14
3	0.914	3	1.035	40.75	0.329	12.97	0.085	132.14
4	1.219	4	1.067	42.00	0.340	13.37	0.091	140.38
5	1.524	5	1.086	42.75	0.346	13.61	0.094	145.43
6	1.829	6	1.118	44.00	0.356	14.01	0.099	154.06

Defects				
Defect No.	Reference Angle	Distance from Top		Description
	(degrees)	(m)	(in.)	
1	0 - 360	0.406	16	Increasing circumference (36" ->41")
2	260	1.778	70	1" dia. hole
3	90	1.778	70	1" dia. hole
4	0		57	Nailhole
5	5	1.524	60	Nailhole
6	355	1.575	62	Nailhole
7	50	1.562	61.5	Nailhole

Summary of Physical Characteristics for Pile No. 29

Dimensions								
Sect. No.	**Distance from Top**		**Circumference**		**Diameter**		**Area**	
	(m)	**(ft.)**	**(m)**	**(in.)**	**(m)**	**(in.)**	**(m^2)**	**(in^2)**
0	0.000	0	1.000	39.38	0.318	12.53	0.080	123.38
1	0.305	1	1.026	40.38	0.326	12.85	0.084	129.72
2	0.610	2	1.041	41.00	0.331	13.05	0.086	133.77
3	0.914	3	1.057	41.63	0.337	13.25	0.089	137.88
4	1.219	4	1.092	43.00	0.348	13.69	0.095	147.14
5	1.524	5	1.118	44.00	0.356	14.01	0.099	154.06
6	1.829	6	1.140	44.88	0.363	14.28	0.103	160.25

Defects				
Defect No.	**Reference Angle**	**Distance from Top**		**Description**
	(degrees)	(m)	(in.)	
1	350	0.940	37	Nailhole
2	275	1.549	61	Scarf 2.5" X 11"
3	260	0.787	31	Nailhole

Summary of Physical Characteristics for Pile No. 30

Dimensions								
Sect.	**Distance from Top**		**Circumference**		**Diameter**		**Area**	
No.	(m)	(ft.)	(m)	(in.)	(m)	(in.)	(m^2)	(in^2)
0	0.000	0	0.965	38.00	0.307	12.10	0.074	114.91
1	0.305	1	0.994	39.13	0.316	12.45	0.079	121.82
2	0.610	2	1.054	41.50	0.336	13.21	0.088	137.05
3	0.914	3	1.054	41.50	0.336	13.21	0.088	137.05
4	1.219	4	1.064	41.88	0.339	13.33	0.090	139.54
5	1.524	5	1.083	42.63	0.345	13.57	0.093	144.58
6	1.829	6	1.114	43.88	0.355	13.97	0.099	153.19

Defects				
Defect	**Reference Angle**	**Distance from Top**		**Description**
No.	(degrees)	(m)	(in.)	
1	0 - 360	0.432	17	Increasing circumference (39" ->42")
2	45	0.686	27	Hole 4" X 1"
3	70	1.676	66	.5" dia. hole
4	255	1.676	66	.5" dia. hole
5	255	1.676	66	Scarf 3" dia. .5" deep
6	100	0.533	21	2.5" dia. knot

Summary of Physical Characteristics for Pile No. 32

Dimensions								
Sect. No.	Distance from Top		Circumference		Diameter		Area	
	(m)	(ft.)	(m)	(in.)	(m)	(in.)	(m^2)	(in^2)
0	0.000	0	1.057	41.63	0.337	13.25	0.089	137.88
1	0.305	1	1.099	43.25	0.350	13.77	0.096	148.86
2	0.610	2	1.111	43.75	0.354	13.93	0.098	152.32
3	0.914	3	1.130	44.50	0.360	14.16	0.102	157.58
4	1.219	4	1.175	46.25	0.374	14.72	0.110	170.22
5	1.524	5	1.213	47.75	0.386	15.20	0.117	181.44
6	1.829	6	1.248	49.13	0.397	15.64	0.124	192.04

Defects				
Defect No.	Reference Angle	Distance from Top		Description
	(degrees)	(m)	(in.)	
1	0 - 360	0.229	9	Increasing circumference (39" ->42")
2	330	0.800	31.5	.5" dia. hole
3	188	1.727	68	1" dia hole
4	180	0.787	31	Nailhole
5	80	0.356	14	Nailhole
6	75	0.457	18	Nailhole
7	350	1.524	60	Nailhole
8	345	1.702	67	.5" dia. hole

This public document is published at a total cost of $908.00 . One hundred and seventy-five copies of this public document were published in this first printing at a cost of $628.00. The total cost of all printings of this document including reprints is $908.00. This document was published by Louisiana State University, Graphic Services, 3555 River Road, Baton Rouge, Louisiana 70802, to report and publish research findings for the Louisiana Transportation Research Center as required in R.S. 48:105. This material was duplicated in accordance with standards for printing by state agencies established pursuant to R.S. 43:31. Printing of this material was purchased in accordance with the provisions of Title 43 of the Louisiana Revised Statutes.

Louisiana Transportation Research Center
4101 Gourrier Avenue
Baton Rouge, Louisiana 70808
Phone (504) 767-9131
FAX (504) 767-9108